New Physics Opportunities in Photon Induced Interactions at the LHC

V. P. Gonçalves [1,2]

[1] Department of Astronomy and Theoretical Physics, Lund University, 223-62 Lund, Sweden.
[2] Instituto de Física e Matemática, Universidade Federal de Pelotas, Caixa Postal 354, CEP 96010-900, Pelotas, RS, Brazil

E-mail: victor.goncalves@thep.lu.se;barros@ufpel.edu.br

Abstract. In the last years the Large Hadron Collider (LHC) at CERN has collected a large amount of data considering pp, pPb and $PbPb$ collisions, which is allowing to probe the Standard Model in a new kinematical range. In this contribution I will show that the LHC can also be considered as a photon collider, which allows to study several aspects of the hadronic physics by the analysis of photon induced interactions in hadronic collisions. The basic idea is that in these interactions the total cross section for a given process can be factorized in terms of the equivalent flux of photons into the hadron projectile and the photon-photon or photon-target production cross section. The main advantages of using hadron - hadron collisions for studying photon induced interactions are the high equivalent photon energies and luminosities that can be achieved at existing accelerators. I review recent results which demonstrated that photon induced interactions at LHC can be used to study the QCD dynamics at high energies, the Odderon, Charmoniumlike Exotic states, and the photon flux of the proton.

1. Introduction

In recent years a series of experimental results at RHIC [1, 2], Tevatron [3] and LHC [4, 5, 6, 7, 8, 9, 10, 11] demonstrated that the study of photon - induced interactions in hadronic colliders is feasible and can be used to probe e.g. the nuclear gluon distribution [12, 13, 14, 15], the dynamics of the strong interactions [16, 17, 18, 19, 20, 21, 22, 23], the Odderon [28, 29], the mechanism of quarkonium production [24, 25, 26, 27, 22, 23] and the photon flux of the proton [30, 31]. It has stimulated the improvement of the theoretical description of these processes as well as the proposal of new forward detectors to be installed in the LHC [32]. The basic idea in the photon-induced processes is that a ultra relativistic charged hadron (proton or nuclei) give rise to strong electromagnetic fields, such that the photon stemming from the electromagnetic field of one of the two colliding hadrons can interact with one photon of the other hadron (photon - photon process) or can interact directly with the other hadron (photon - hadron process) [33, 34]. In these processes the total cross section can be factorized in terms of the equivalent flux of photons into the hadron projectile and the photon-photon or photon-target production cross section. In the case of photon-hadron interactions, they can be divided into exclusive and inclusive reactions. In the first case, a certain particle is produced while the target remains in the ground state (or is only internally excited). On the other hand, in inclusive interactions the particle produced is accompanied by one or more particles from the breakup of the target. Since photon emission is coherent over the entire nucleus and the photon is colorless we have

that the inclusive events are characterized by one rapidity gap, while two rapidity gaps should be present in the final state of the exclusive processes. The typical examples of these processes are the exclusive vector meson production, described by the process $\gamma h \to Xh$ ($X = \rho, J/\Psi, \Upsilon$), and the inclusive heavy quark production [$\gamma h \to XY$ ($X = c\overline{c}, b\overline{b}, t\overline{t}$)], respectively. The cross section for the photoproduction of a final state X in a hadronic collision is given by,

$$\sigma(h_1 h_2 \to h_3 XY) = \sum_{i=1,2} \int dY \frac{d\sigma_i}{dY}\,, \tag{1}$$

where h_3 is identical to the initial state hadron that emitted the photon, X represents the produced final state and the system Y is the other initial state hadron in the case of exclusive processes or a multi - state system in the case of inclusive processes. Moreover, $d\sigma_i/dY$ is the rapidity distribution for the photon-target interaction induced by the hadron h_i ($i = 1, 2$), which can be expressed as

$$\frac{d\sigma_i}{dY} = x\gamma_i(x, \mu^2)\, \sigma_{\gamma h_j \to X h_3}(W^2_{\gamma h_j}) \quad (i \neq j)\,, \tag{2}$$

where x is the fraction of the hadron energy carried by the photon, $\gamma_i(x, \mu^2)$ is the equivalent flux of photons of the hadron projectile and μ has to be identified with a momentum scale of the photon - induced process. Moreover, $W^2_{\gamma h} = 2\,\omega\sqrt{s_{\rm NN}}$ and $s_{\rm NN}$ are the c.m.s energy squared of the photon - hadron and hadron-hadron system, respectively, with ω being the photon energy. It is important to emphasize that for a nuclei the elastic component of the photon flux is proportional to squared charge of the hadron (Z^2), due to the coherent action of all protons in the nucleus. One of the main advantages of using colliding hadrons and nuclear beams for studying photon induced interactions is the high equivalent photon energies and luminosities that can be achieved at existing and future accelerators (For a review see Ref. [33]). For example, if we consider $pp/pPb/PbPb$ collisions at LHC, the Lorentz factor is $\gamma_L = 7455/4690/2930$, giving the maximum c.m.s. γN energy $W_{\gamma p} \approx 8390/1500/950$ GeV. Therefore, while studies of photoproduction at HERA were limited to photon-proton center of mass energies of about 300 GeV, photon-hadron interactions at LHC reach one order of magnitude higher on energy. Consequently, studies of γh interactions at the LHC could provide valuable information on the strong interactions theory in a kinematical which have been not probed utterly.

Our goal in this contribution is to demonstrate that photon induced interactions at the LHC are an important laboratory for the study of hadronic physics, which allows to probe several aspects which remain open questions in the Standard Model. In particular, I will discuss the possibility to probe the gluon distribution at small - x (Section 2), the QCD dynamics (Section 3), the Odderon (Section 4), the production of charmoniumlike exotic states (Section 5) and the photon flux of the proton (Section 6). Finally, in Section 7 we summarize our main conclusions.

2. Probing the gluon distribution at small-x

A systematic measurement of the gluon distribution of thea hadrons (protons and nuclei) is of fundamental interest in understanding the parton structure of hadrons, to determine the initial conditions of the quark gluon plasma (QGP) predicted to be formed in central heavy ion collisions, and to probe the QCD dynamics at high energies which implies a modification of the gluon dynamics [35]. During the last years, our understanding about the gluon distribution of the proton have largely improved by the analysis of the ep HERA data, but several questions still remains open. In contrast, the behaviour of the nuclear gluon distribution is completely undetermined by the fixed target experiments. In the last years several groups [36, 37, 38, 39, 40] have proposed parametrizations for the nuclear parton distributions (nPDF), which are based on different assumptions and techniques to perform a global fit of different sets of data using the

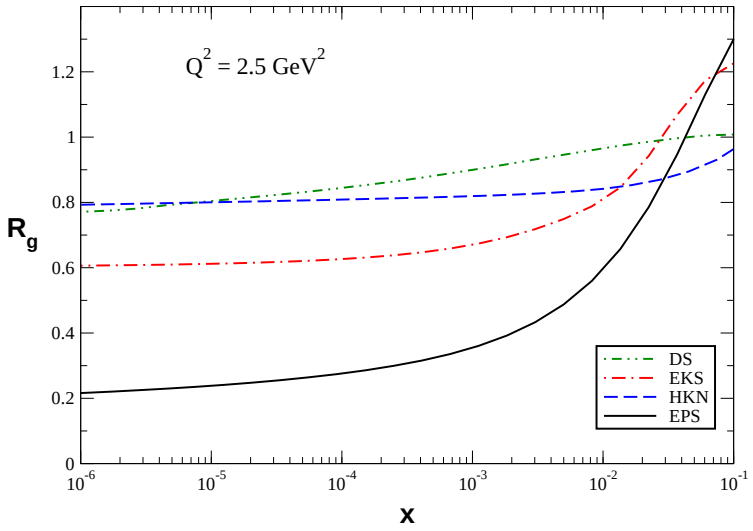

Figure 1. (Color online) Ratio $R_g \equiv xg_A/A.xg_N$ predicted by the DS [37], EKS [36], HKN [39] and EPS [40] parametrizations at $Q^2 = 2.5$ GeV^2 and $A = 208$.

DGLAP evolution equations (For details see, e.g., Ref. [41]). Due to the scarce experimental data in the small-x region and/or for observables strongly dependent on the nuclear gluon distribution, the current status is that its behaviour is completely undefined. It is demonstrated by the analysis of the Fig. 1, where we present the results for the ratio $R_g \equiv xg_A/A.xg_N$ predicted by the EKS [36], DS [37], HKN [39] and EPS [40] parametrizations at $Q^2 = 2.5$ GeV^2 and $A = 208$. It is important to emphasize that the EPS group has release in 2009 a new parametrization (EPS09) [42] which predicts a smaller amount of gluon shadowing, with a behaviour closer to the EKS one. As we can see, these parametrizations predict very distinct magnitudes for the nuclear effects. For larger values of x, the EKS and the EPS show antishadowing, while this effect is absent for the HKN and EPS parametrizations in the $x \leq 10^{-1}$ domain. The more surprising feature is however the amount of shadowing in the different parametrizations. While the shadowing is moderate for DS and HKN parametrizations and somewhat bigger for EKS one, the EPS prediction has a much stronger suppression compared with the other parametrizations. For smaller x around $x \simeq 10^{-5}$, while DS and HKN parametrizations have about 20% suppression and EKS one have about 40% suppression, for the EPS parametrization this effect goes to almost 80% suppression in the nuclear gluon compared with the A scaled gluon content in the proton! For bigger values of x the behaviour is distinct for all parametrizations. As x grows, the DS parametrization predicts that R_g grows continuously to 1, that means that the shadowing dies out when $x \to 10^{-1}$. The same happens for the HKN one in this limit, but this growth starts only at $x > 10^{-2}$, with R_g being flat for $10^{-5} < x < 10^{-2}$. At $x \approx 10^{-1}$, we have that behaviours predicted by the EKS and EPS parametrizations are similar, with R_g exceeding 1.2. The main distinction between these parametrizations is that in the EPS parametrization one has a much steeper growth, from a much stronger suppression at smaller x to the antishadowing behaviour for larger values of x. Our understanding about the nuclear gluon distribution should be improved in the future electron-nucleus colliders. However, as the date of construction and start of operation of these colliders is still in debate, we need to obtain alternative searches to estimate the medium effects in the nuclear gluon distribution. It has motivated several authors to propose the study of different observables in distinct processes to constrain the nuclear gluon distribution. One possibility is the study of the heavy quark

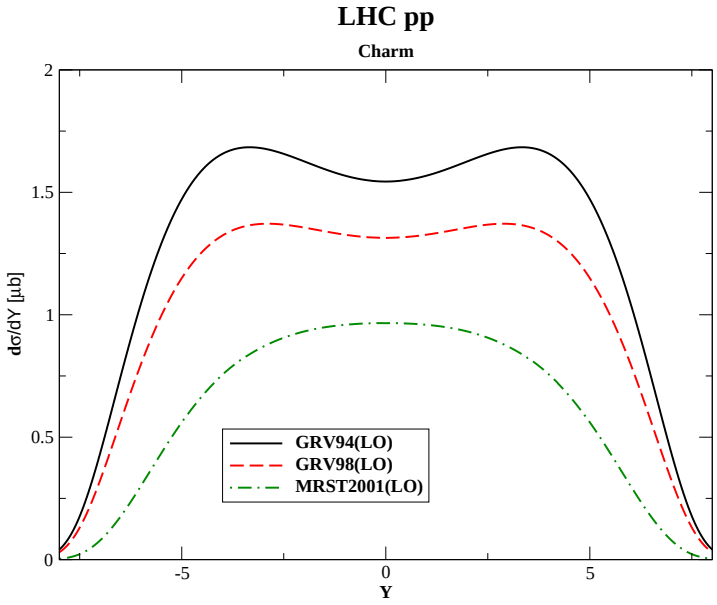

Figure 2. (Color online) Predictions for the rapidity distribution for the photoproduction of charm quarks in pp collisions at LHC ($\sqrt{s} = 14$ TeV).

photoproduction in hadronic collisions, which is an inclusive processes, characterized by one rapidity gap in the final state. In this case, the cross section is directly proportional to the target gluon distribution, which makes the analysis of the rapidity distribution a direct probe of the gluon distribution for different values of the Bjorken - x variable. This processes have been analysed by several authors in the last years [12, 14, 43, 44, 45, 46] and some recent results will be revised in the subsection 2.1. Another alternative to constrain the gluon distribution is the study of exclusive processes in hadronic collisions, which are characterized by two rapidity gaps in the final state. In particular, in Ref. [12] we have proposed by the first time the study of vector meson photoproduction in ultraperipheral heavy ion collisions at RHIC and LHC in order to constrain the nuclear medium effects present in the nuclear gluon distribution. As the cross section for the diffractive vector meson production depends (quadratically) on the gluon distribution, it gives a unique opportunity to study the low x behaviour of the gluons inside the nucleus. In subsection 2.2 we will present a brief results of the formalism and show some results which demonstrate that this process is the ideal scenario to constrain the gluon distribution.

2.1. Probing the gluon distribution in inclusive processes

Heavy quark production in hard collisions has been considered as a clean test of perturbative Quantum Chromodynamics (QCD) (For a review see, e.g., Ref [47]). This process provides not only many tests of perturbative QCD, but also some of the most important backgrounds to new physics processes, which have motivated an extensive phenomenology at DESY-HERA, Tevatron and LHC. These studies are mainly motivated by the strong dependence of the cross section on the behaviour of the gluon distribution, which determines the QCD dynamics at high energies. In particular, the charm and bottom photoproduction on nucleon and nuclei targets has been studied in detail in, e.g., Ref. [48], considering the several available scenarios for the QCD dynamics at high energies. The results of those analysis show that future electron-proton (nucleus) colliders, probably could determine the behaviour of the gluon distribution at small values of the Bjorken-x variable. Along these lines, in Refs. [49, 13, 45] we have analysed the

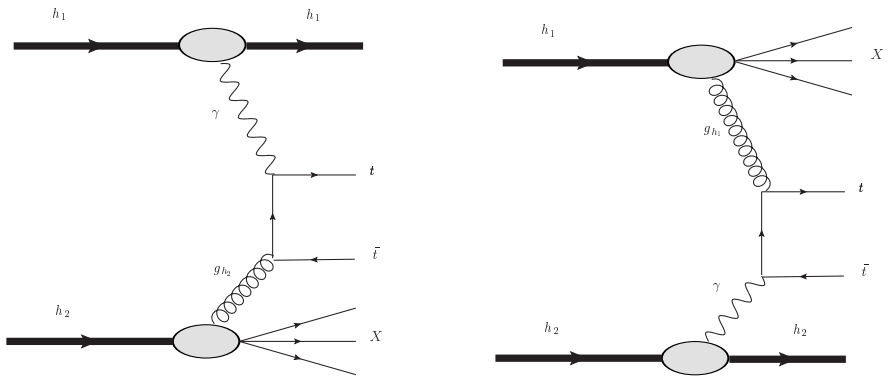

Figure 3. The mechanism for the photoproduction of top quarks in coherent hadron - hadron interactions.

possibility of using the LHC as a photon - hadron collider and studied the bottom and charm production assuming distinct formalisms for the QCD evolution (For more recent studies see [14]). In particular, in Ref. [45] we have demonstrated that the study of charm photoproduction in pp collisions can be used to constrain the gluon distribution of the proton, since the rapidity distribution is strongly dependent on the model used for the gluon density and its behaviour at small-x, as shown in Fig. 2.

In Ref. [46] we have extended these previous analysis on heavy quark photoproduction for the case of the top quark, which play a special role in the Standard Model, in particular in the electroweak symmetry breaking. Precise measurements of its properties and interactions may also reveal effects from new physics (For a recent review see Ref. [50]). Although several properties of the top quark have been examined in the last eighteen years at the Tevatron, the collected statistics was small. In contrast, they are largely produced at the LHC. Our goal in Ref. [46] was to verify if the photoproduction of top quarks in coherent interactions at LHC could also be used to improve our knowledge of its properties (For previous studies see Ref. [33]). The basic diagrams for the photoproduction of top quarks in coherent hadron - hadron interactions are represented in Fig. 3. It is important to emphasize that the photoproduction of top quarks was not studied in the HERA ep collider and its experimental analysis still is an open question, which also have motivated the study of the production of top quarks in coherent interactions. In what follows we will present a brief review of the main results obtained in Ref. [46].

The main input for the calculation of the top photoproduction in hadronic collisions is the photon-proton cross section, which can be estimated considering different theoretical scenarios [49]. In Ref. [46] we have considered the collinear factorization approach, where the cross sections involving incoming hadrons are given, at all orders, by the convolution of intrinsically non-perturbative, but universal, quantities - the parton densities, with perturbatively calculable hard matrix elements, which are process dependent. In this approach, all partons involved are assumed to be on mass shell, carrying only longitudinal momenta, and their transverse momenta are neglected in the QCD matrix elements. In particular, the cross section for the photoproduction of heavy quarks is given in terms of the convolution between the elementary cross section for the subprocess $\gamma g \to Q\overline{Q}$ and the probability of finding a gluon inside the hadron, namely the gluon distribution. At leading order, the top quark photoproduction cross

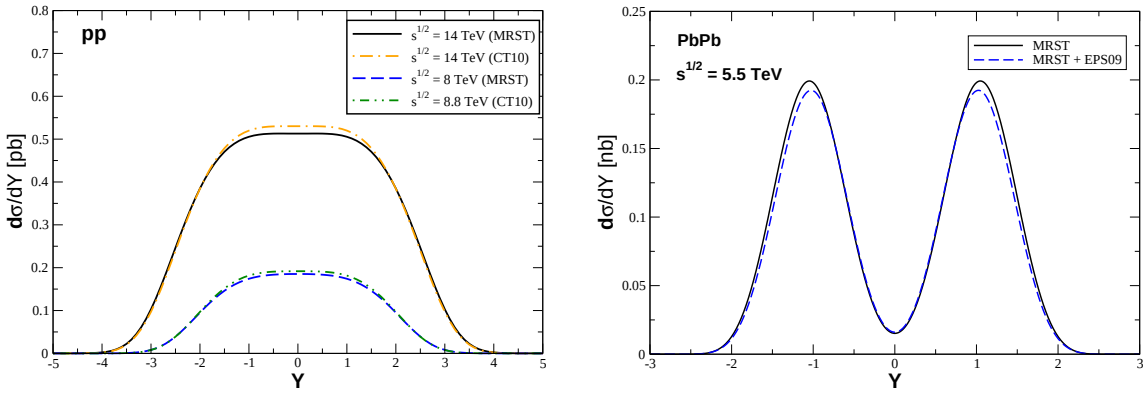

Figure 4. (Color online) Predictions for the rapidity distribution for the photoproduction of top quarks in pp (left panel) and $PbPb$ (right panel) collisions at LHC.

section is given by [51],

$$\sigma_{\gamma h \to t\bar{t}X}(W_{\gamma h}) = 4\,\pi\, e_t^2 \int_{4m_t^2}^{W_{\gamma h}^2} \frac{dM_{t\bar{t}}^2}{M_{t\bar{t}}^4}\, \alpha_{em}\alpha_s(\mu_F^2)\, x g_h(x,\mu_F^2) \times \left[\left(1+\beta-\frac{1}{2}\beta^2\right) \ln\left(\frac{1+\sqrt{1-\beta}}{1-\sqrt{1-\beta}}\right) - (1+\beta)\sqrt{1-\beta}\right] , \quad (3)$$

where $M_{t\bar{t}}$ is the invariant mass of the top quark pair, with $x = M_{t\bar{t}}^2/W_{\gamma h}^2$, and $g_h(x,\mu_F^2)$ is the gluon density inside the hadron at the factorization scale μ_F^2. In addition, m_t is the top quark mass, e_t is its electric charge and $\beta \equiv 4\,m_t^2/M_{t\bar{t}}^2$. In our calculations we have used $\mu_F^2 = 4\,m_t^2$, with $m_t = 173.0$ GeV. It should be noticed that different choices for the factorization scale and quark mass produce distinct overall normalization to the total cross section at photon-nucleon interactions and that NLO corrections, which are small in comparison to the hadroproduction case, can be absorbed in these redefinitions of μ_F^2 and m_t^2 [52]. In Ref. [46] we have considered different parametrizations for the parton distributions. In particular, we used the MRST [53] and CT10 [54] parton distributions for the proton. In the nuclear case, we take into account the nuclear shadowing effects as given by the EPS09 parametrization [42], which is based on a global fit of the current nuclear data. Before to present the results, it is important to emphasize the typical values of x which will be probed in coherent $pp/pPb/PbPb$ collisions. Considering that for $pp/pPb/PbPb$ collisions at LHC the Lorentz factor is $\gamma_L = 7455/4690/2930$ [33], we obtain that the maximum c.m.s. γh energy will be $W_{\gamma h} \approx 8390/1500/950$ GeV. Consequently, we obtain that for the top quark photoproduction in coherent interactions, we will probe the gluon distribution at $x > 1.7 \times 10^{-3}$ in pp collisions, $x > 5.3 \times 10^{-2}$ in pPb collisions and $x > 0.13$ in $PbPb$ collisions.

In Fig. 4 we present the predictions obtained in Ref. [46] for pp and $PbPb$ collisions at LHC energies. As expected, the total rapidity distributions are symmetric about the midrapidity. In the case of pp collisions, we calculated $d\sigma/dY$ considering different parametrizations for the gluon distribution in the proton. We can see in the Fig. 4 (left panel) that the MRST and CT10 predictions are similar, with the MRST one being a lower bound. In Table 1 we present the estimates for the total cross sections and production rates assuming the design luminosity $\mathcal{L}_{\rm LHC}^{\rm pp} = 10^7$ mb^{-1}s^{-1} and a run time of 10^7 seconds. We predict large values for the events rate and cross sections of the order of units of pb, in contrast with values of the order of 160 pb for the inclusive top quark pair hadroproduction [50]. Despite their much smaller

pp	**MRST**	**CT10**
$\sqrt{s} = 8$ TeV	0.739 pb (73900)	0.764 pb (76400)
$\sqrt{s} = 14$ TeV	2.50 pb (250000)	2.53 pb (253000)
pPb	**MRST**	**MRST + EPS09**
$\sqrt{s} = 5.5$ TeV	0.036 nb (5.4/3600)	0.038 nb (5.7/3800)
$\sqrt{s} = 8.8$ TeV	0.159 nb (23.85/15900)	0.165 nb (24.75/16500)
PbPb	**MRST**	**MRST + EPS09**
$\sqrt{s} = 5.5$ TeV	0.42 nb (0.18)	0.40 nb (0.17)

Table 1. The integrated cross section (events rate) for the photoproduction of top quarks in pp, pPb and $PbPb$ collisions at LHC energies.

cross sections, the clean topology of coherent processes implies a larger signal to background ratio. Therefore, the experimental detection is in principle feasible. However, it is important to emphasize that the signal is expected to be reduced due to the event pileup. An alternative to measure coherent events at the LHC is by tagging the intact hadron in the final state. Such possibility is currently under study (See e.g. [32]). In Fig. 4 (right panel) we present our results for $PbPb$ collisions. In our calculations we consider that the nuclear gluon distribution is given by $xg_A = A.R_g.xg_p$, where R_g takes into account the nuclear shadowing effects as given by the EPS09 parametrization [42] and xg_p is the proton gluon distribution, given by the MRST parametrization [53]. We denote by MRST+EPS09 the predictions obtained including the shadowing effects and by MRST those obtained disregarding these effects, i.e., with $R_g = 1$. We can see that the total cross section is reduced by $\approx 5\%$ by the EMC effect present in the EPS09 parametrization for large values of $x\,(\geq 0.4)$, which implies $R_g < 1$. This small contribution of the shadowing effects is expected due to the large value of the hard scale $(= 4m_t^2)$ present in the process. Moreover, distinctly from the pp case, $d\sigma/dY$ is small at $Y \approx 0$ and is almost null at $Y \geq 2$. It is directly associated to the distinct large - ω behaviours of the proton and nuclear photon fluxes, with the latter being exponentially suppressed at $\omega > 80$ GeV while the photon flux of the proton extends up to $\omega \approx 2400$ GeV. Moreover, in Table 1 we present our estimates for the total cross sections and production rates assuming the design luminosity $\mathcal{L}_{\rm LHC}^{\rm PbPb} = 0.42$ mb^{-1}s^{-1} and a run time of 10^6 seconds. Our results indicate that for the default settings and running time, the statistics is marginal for $PbPb$ collisions. In Table 1 we also present our estimates for the total cross sections and production rates for pPb collisions assuming the design luminosity $\mathcal{L}_{\rm LHC}^{\rm pPb} = 150$ mb^{-1}s^{-1} and a run time of 10^6 seconds. We predict cross sections that are a factor three smaller than those obtained in the $PbPb$ case. The larger pA luminosity, which is two order of magnitude higher than for AA, counteracts this suppression for the event rates. However, the resulting events rates still are small. Recently, an upgraded pPb scenario was proposed in Ref. [55], which improve the pPb luminosity and the running time. These authors proposed the following scenario for pPb collisions: $\mathcal{L}^{\rm pPb} = 10^4$ mb^{-1}s^{-1} and a run time of 10^7 s. The corresponding event rates also are presented in the Table 1. In this case we have reasonable numbers, which makes the experimental analysis feasible. Another advantage of pPb collisions is that it is expected to trigger on and carry out the measurement with almost no pileup [55]. Therefore, the upgraded pA scenario provides one of the best possibilities to detect the top quark in coherent processes.

2.2. Probing the gluon distribution in exclusive processes

In the collinear formalism, based on the QCD factorization theorem [56], the cross section for the vector meson production off any hadronic target, including a nucleus, at small-x and for a

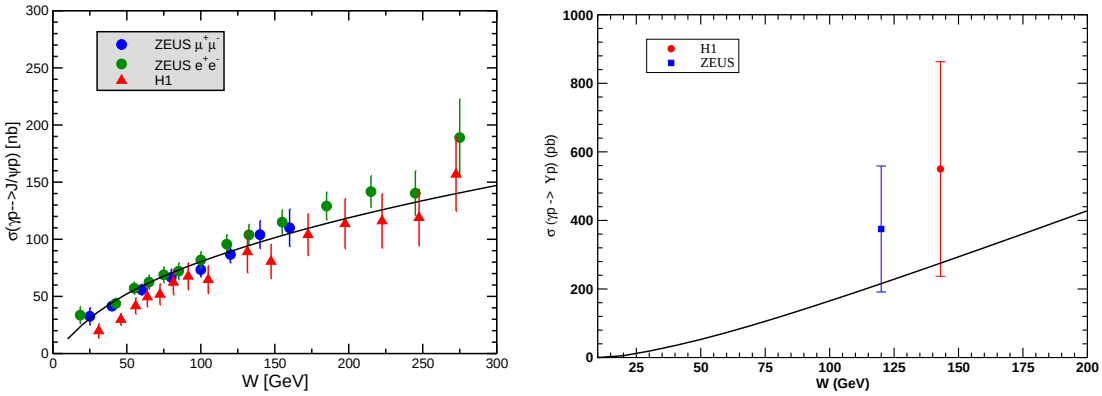

Figure 5. (Color online) Energy dependence of the exclusive J/Ψ (left panel) and Υ (right panel) photoproduction cross section. Comparison with HERA data [64, 65, 66].

sufficiently hard scale, is proportional to the square of the gluon parton density of the target. To lowest order, the $\gamma h \to Vh$ ($h = p$, A) amplitude can be factorized into the product of the $\gamma \to Q\overline{Q}$ transition ($Q = c$, b), the scattering of the $Q\overline{Q}$ system on the target via (colorless) two-gluon exchange, and finally the formation of the quarkonium from the outgoing $Q\overline{Q}$ pair. The heavy meson mass M_V ensures that perturbative QCD can be applied to photoproduction. The calculation was performed some years ago to leading logarithmic ($\log(\overline{Q}^2)$) approximation, assuming the produced vector meson quarkonium system to be nonrelativistic [57, 58] and improved in distinct aspects [59, 60]. Assuming a non-relativistic wave function for the vector meson one have that the $t = 0$ differential cross section of photoproduction of heavy vector mesons in leading order collinear approximation is given by [57, 58]

$$\frac{d\sigma(\gamma h \to Vh)}{dt}|_{t=0} = \frac{\pi^3 \Gamma_{ee} M_V^3}{48\alpha} \frac{\alpha_s^2(\overline{Q}^2)}{\overline{Q}^8} \times [x g_h(x, \overline{Q}^2)]^2 \ , \tag{4}$$

where xg_h is the target gluon distribution, $x = 4\overline{Q}^2/W^2$ with W the center of mass energy and $\overline{Q}^2 = M_V^2/4$. Moreover, Γ_{ee} is the leptonic decay width of the vector meson. The strong dependence on xg offers an opportunity to use the experimental HERA data for the $\gamma^* p \to J/\Psi p$ process to determine the behaviour of the gluon distribution at low x and in the Q^2 region, which is not constrained by the global analyses [61]. In Refs. [59, 60, 61, 63, 62] the authors have estimated the relativistic corrections [$\mathcal{O}(4\%)$] , the real part contribution of the production amplitude [$\mathcal{O}(15\%)$], the effect of off-diagonal partons [$\mathcal{O}(20\%)$] and next-to-leading order corrections [$\mathcal{O}(40\%)$] to the LO exclusive heavy vector meson production, given by Eq. (4).

In order to obtain a baseline for the calculations of the vector meson production in γA interactions, in Ref. [13] we have initially estimated the γp cross section and compared it with the HERA data. Following Refs. [63, 61] we have estimated the total cross section for the J/Ψ and Υ photoproduction at HERA using the MRST(LO) parametrization [53] for the nucleon gluon distribution and including the corrections discussed above. Moreover, we have considered an exponential parametrization for the small $|t|$ behaviour of the amplitude e assumed $b = 4.5$ GeV^{-2} as in Refs. [59, 61]. In Fig. 5 we present a comparison between our predictions and the J/Ψ (left panel) and Υ (right panel) HERA data [64, 65, 66], which demonstrated that it are reasonably described. In Ref. [13] we have assumed that the corrections for the LO exclusive heavy vector meson production are independent of the target. Moreover, we assumed that in

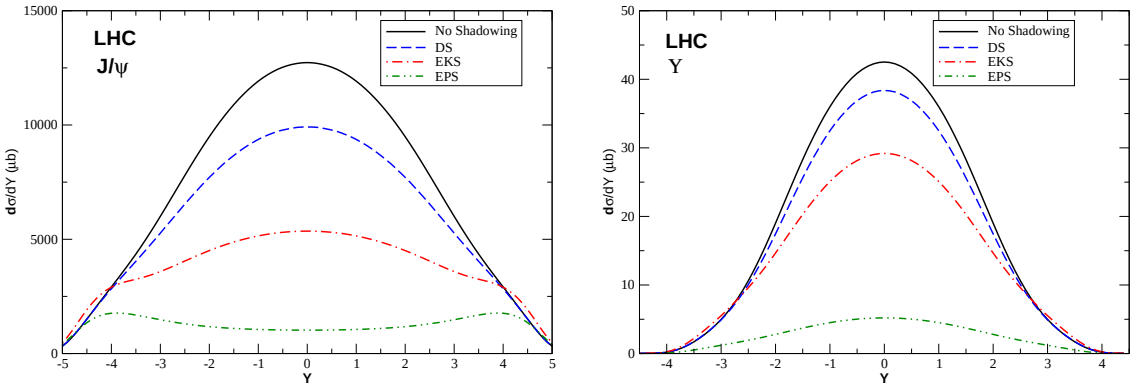

Figure 6. (Color online) The rapidity distribution for nuclear vector meson photoproduction on UPC's in AA reactions at LHC energy ($\sqrt{S_{NN}} = 5.5\,\mathrm{TeV}$).

the case of nuclear targets, b is dominated by the nuclear size, with $b \sim R_A^2$ and the non-forward differential cross section is dominated by the nuclear form factor, which is the Fourier transform of the nuclear density profile. Therefore, we have considered that the total cross section for vector meson production in γA interactions is given by

$$\sigma(\gamma A \to V A) = \frac{d\sigma(\gamma A \to V A)}{dt}|_{t=0} \int_{t_{min}}^{\infty} dt\, |F(t)|^2 \;\; , \tag{5}$$

where $t_{min} = (M_V^2/2\omega)^2$ and $F(t) = \int d^3r\ \rho(r)\ \exp(i\mathbf{q}\cdot\mathbf{r})$ is the nuclear form factor for the distribution. The main input in the calculations of the quarkonium photoproduction cross section in the collinear formalism is the nuclear gluon distribution. The difference between the distinct parametrizations observed in Fig. 1 will be amplified in the exclusive quarkonium photoproduction in γA interactions due to the quadratic dependence on xg_A of the cross section. Consequently, it is expected a large difference between the predictions obtained using the distinct parametrizations. This was the main motivation for the calculations presented in Ref. [13] (See also Ref. [14]).

In what follows we present a brief review of the main results obtained in Ref. [13], where we have calculated the rapidity distributions and total cross sections for quarkonium production in ultraperipheral heavy ion collisions at RHIC and LHC energies. We have assumed that $xg_A(x,Q^2) = R_g(x,Q^2).A\,xg_p(x,Q^2)$, with R_g given by the DS, EKS and EPS parametrizations and xg_p given by the MRST(LO) parametrization [53]. As the HKN parametrization is similar to the DS one in the kinematical range considered, it was not included in our analyses. In Fig. 6 we present our predictions for J/Ψ (left panel) and Υ (right panel) production in coherent AA collisions, considering $A = Pb$ and $\sqrt{s_{NN}} = 5.5$ TeV. The production at mid-rapidity at the LHC probes x-values of order $(6-20)\times 10^{-4}$, where the nuclear parametrizations differ by a factor 4 (See Fig. 1). The no shadowing prediction is presented for comparison. At LHC energies the rapidity distribution is strongly dependent of the magnitude of the shadowing effects in the nuclear gluon distribution. While the DS prediction implies a small reduction at mid-rapidity in comparison to the no shadowing one, the rapidity distribution is suppressed by a factor 10 if calculated using the EPS gluon. Moreover, as the difference between the predictions of the three parametrizations is very large, in Ref. [13] we have concluded that the rapidity distribution for exclusive quarkonium photoproduction in UPC's at LHC could be used to constrain the magnitude of the shadowing effect. Such conclusion was recently confirmed by the experimental results from the ALICE Collaboration for $\sqrt{s} = 2.76$ TeV [4].

3. Probing the QCD dynamics at high energies

The description of QCD dynamics in the high energy limit still is a subject of intense debate (For a review see e.g. Refs. [35, 67]). Theoretically, at high energies (small Bjorken-x) one expects the transition of the regime described by the linear dynamics (denoted Low Density QCD in Fig. 7), where only the parton emissions are considered, to a new regime where a high gluon density is present and the physical process of recombination of gluons becomes important in the parton cascade, with the evolution being given by a non linear evolution equation. This high density QCD regime is characterized by the limitation on the maximum phase-space parton density that can be reached in the hadron wave function (gluon saturation), with the transition between the low and high density regimes being specified by the saturation scale $Q_{\rm s}$ [67] (See Fig. 7). Currently, the state of art formalism to describe the gluon saturation effects is the Colour Glass Condensate [69]. In this formalism the non linear and quantum effects in the hadron wave function are encoded in the imaginary part of the forward amplitude for the scattering between a small dipole (a colorless quark-antiquark pair) and a dense hadron target, at a given rapidity interval $Y = \ln(1/x)$, which is represented by $\mathcal{N}(\boldsymbol{b}, \boldsymbol{r}, x)$. This quantity is directly related to the dipole - hadron cross section, σ_{dip}, which encodes all the information about the hadronic scattering, as follows

$$\sigma_{dip}(\boldsymbol{r}, x) = 2 \int d^2b \mathcal{N}(\boldsymbol{b}, \boldsymbol{r}, x). \tag{6}$$

The dipole has transverse size given by the vector $\boldsymbol{r} = \boldsymbol{x} - \boldsymbol{y}$, where $\boldsymbol{x}$ and $\boldsymbol{y}$ are the transverse vectors for the quark and antiquark, respectively, and impact parameter $\boldsymbol{b} = (\boldsymbol{x} + \boldsymbol{y})/2$. At high energies the evolution with the rapidity Y of $\mathcal{N}(\boldsymbol{r}, \boldsymbol{b}, Y)$ is given by the infinite hierarchy of equations, the so called Balitsky-JIMWLK equations [68, 69], which reduces in the mean field approximation to the Balitsky-Kovchegov (BK) equation [68, 70]. It is useful to assume the translational invariance approximation, which regards hadron homogeneity in the transverse plane. It implies that the dipole-proton cross section reads $\sigma_{dip}(\boldsymbol{r}, x) = \sigma_0 \mathcal{N}(\boldsymbol{r}, x)$, where the constant σ_0, which results from the $\boldsymbol{b}$ integration, sets the normalization. Moreover, the amplitude becomes independent of the impact parameter $\boldsymbol{b}$ and depends only on the dipole size $r = |\boldsymbol{r}|$. Although a complete analytical solution of the BK equation is still lacking, its main properties are known: (a) for the interaction of a small dipole ($r \ll 1/Q_{\rm s}$), $\mathcal{N}(r) \approx r^2$, implying that this system is weakly interacting; (b) for a large dipole ($r \gg 1/Q_{\rm s}$), the system is strongly absorbed and therefore $\mathcal{N}(\boldsymbol{r}) \approx 1$. The typical momentum scale, $Q_{\rm s}^2 \propto x^{-\lambda}$ ($\lambda \approx 0.3$), is the so called saturation scale. This property is associated to the large density of saturated gluons in the hadron wave function. Experimentally, possible signals of parton saturation have already been observed in ep deep inelastic scattering at HERA, deuteron-gold collisions at RHIC and hadronic collisions at LHC. Although the geometrical scaling and the diffractive events observed at HERA, as well as the high-p_T suppression observed at RHIC, have a natural interpretation in terms of the saturation physics, none of these phenomena can be taken as a conclusive evidence for a new regime of the QCD dynamics. This is due to the kinematical limitations of the experiments. Consequently, the observation of this new regime still needs confirmation and so there has been an active search for new experimental signatures. A decade ago, in Ref. [16] we have proposed by the first time the study of the vector meson photoproduction in hadronic collisions as a probe of the QCD dynamics. This idea has stimulated the improvement of the theoretical description of this process, which have been done by our group [17, 18, 25, 26, 22, 23] and several other authors [19, 20, 21, 24, 27] in the last years, with its predictions describing very well the recent experimental data. In what follows we will present a brief review of the recent results obtained in the Refs. [22, 23].

Lets consider the description of the vector meson photoproduction in the color dipole formalism [71], with its production in hadronic collisions being represented in Fig. 8. At high energies color dipoles with a defined transverse separation are eigenstates of the interaction

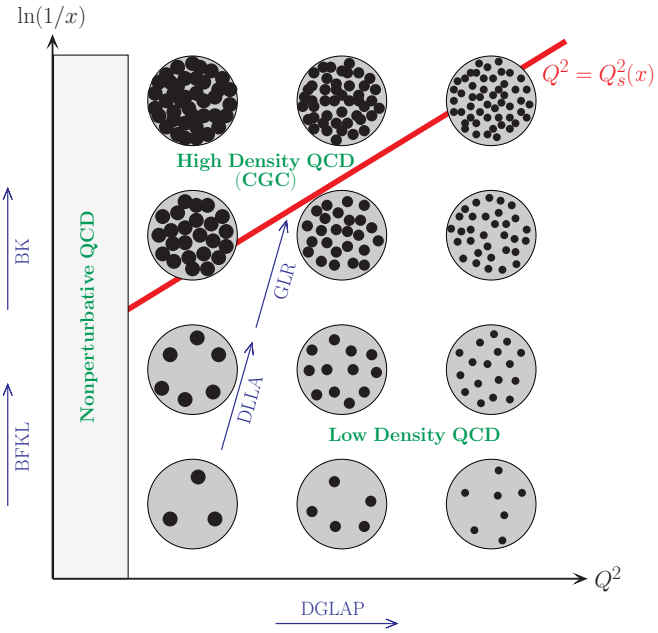

Figure 7. (Color online) Representation of the QCD evolution in the kinematical plane.

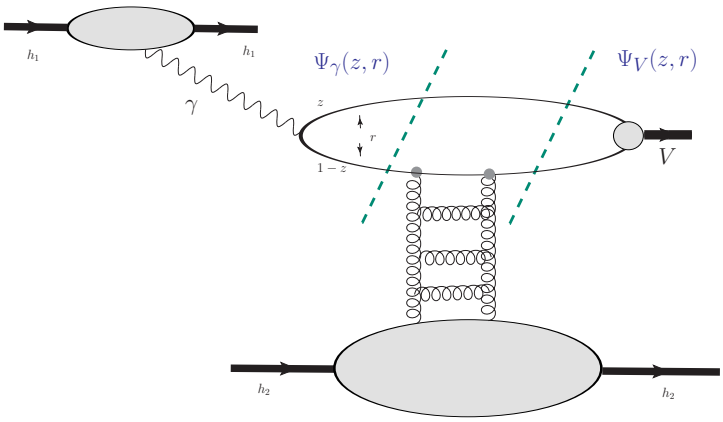

Figure 8. (Color online) Exclusive vector meson photoproduction in hadronic collisions.

with the main quantity of this formalism being the dipole-target cross section. In particular, it provides a unified description of inclusive and diffractive observables in lepton - hadron processes as well as for in Drell-Yan, prompt photon and heavy quark production in hadron-hadron collisions. Furthermore, an important advantage of this formalism is that it is very simple to include nuclear effects. In the color dipole formalism the γh scattering is described in the dipole frame, in which most of the energy is carried by the hadron, while the photon has just enough energy to dissociate into a quark-antiquark pair before the scattering. In this representation the probing projectile fluctuates into a quark-antiquark pair (a dipole) with transverse separation $\boldsymbol{r}$ long before the interaction, which then scatters off the hadron [71]. In this formalism, the scattering amplitude for the diffractive photoproduction of an exclusive final state, such as a

vector meson V ($= J/\Psi$ or Υ), in a γp collision is given by (See e.g. Refs. [71, 16, 72, 73])

$$\mathcal{A}^{\gamma p\to Vp}(x,\Delta) = i\int dz\, d^2\boldsymbol{r}\, d^2\boldsymbol{b} e^{-i[\boldsymbol{b}-(1-z)\boldsymbol{r}].\boldsymbol{\Delta}}\ (\Psi_V^*\Psi)\ 2\mathcal{N}_p(x,\boldsymbol{r},\boldsymbol{b}) \tag{7}$$

where $(\Psi_\Upsilon^*\Psi)$ denotes the overlap of the photon and vector meson transverse wave functions. The variable z $(1-z)$ is the longitudinal momentum fraction of the quark (antiquark), Δ denotes the transverse momentum lost by the outgoing proton ($t=-\Delta^2$) and x is the Bjorken variable. The variable $\boldsymbol{b}$ is the transverse distance from the center of the target to the center of mass of the $q\bar{q}$ dipole and the factor in the exponential arises when one takes into account non-forward corrections to the wave functions [74]. Moreover, $\mathcal{N}_p(x,\boldsymbol{r},\boldsymbol{b})$ denotes the non-forward scattering amplitude of a dipole of size $\boldsymbol{r}$ on the proton, which is directly related to the QCD dynamics, as discussed above. The differential cross section for exclusive vector photoproduction is given by

$$\frac{d\sigma}{dt}(\gamma p\to Vp) = \frac{1}{16\pi}|\mathcal{A}^{\gamma p\to Vp}(x,\Delta)|^2\,(1+\beta^2)\,R_g^2\,, \tag{8}$$

where β is the ratio of real to imaginary parts of the scattering amplitude and R_g is the skewness factor, which is associated to the fact that the gluons attached to the $q\bar{q}$ pair can carry different light-cone fractions x, x' of the proton. Moreover, β can be calculated using dispersion relations, being given by $Re\mathcal{A}/Im\mathcal{A} = \tan(\pi\lambda_e/2)$. The total cross section is given by

$$\sigma(\gamma p\to Vp) = \int_{-\infty}^{0}\frac{d\sigma}{dt}\,dt\ . \tag{9}$$

In Ref. [23], we also have calculated the total cross section for the Υ production considering an approximation frequently used in the literature, in which an exponential Ansatz for the t-dependence is assumed for the differential cross section, which implies that

$$\sigma(\gamma p\to Vp) = \frac{1}{B_V}\ \left.\frac{d\sigma}{dt}\right|_{t=0} \tag{10}$$

where B_V is the slope parameter.

In order to estimate the total cross section we need to specify the overlap function $(\Psi_V^*\Psi)$ and the non-forward scattering amplitude $\mathcal{N}(x,\boldsymbol{r},\boldsymbol{b})$. Initially let us discuss the models used for the overlap function. In contrast to the photon wave function, which is well known in the literature (See e.g. [72]), the description of the vector wave functions still is an open question. The simplest approach is to assume that the vector meson is predominantly a quark-antiquark state and that the spin and polarization structure is the same as in the photon [75, 76, 77, 78]. As a consequence, the overlap between the photon and the vector meson wave function, for the transversely polarized case, is given by (For details see Ref. [72])

$$(\Psi_V^*\Psi)_T = \hat{e}_f e\frac{N_c}{\pi z(1-z)}\left\{m_f^2 K_0(\epsilon r)\phi_T(r,z) - [z^2+(1-z)^2]\epsilon K_1(\epsilon r)\partial_r\phi_T(r,z)\right\}\ , \tag{11}$$

where $\hat{e}_f$ is the effective charge of the vector meson, m_f is the quark mass, $N_c = 3$, $\epsilon^2 = z(1-z)Q^2 + m_f^2$ and $\phi_T(r,z)$ define the scalar part of the vector meson wave function. In what follows we will consider the Boosted Gaussian and Gauss-LC models for $\phi_T(r,z)$, which are largely used in the literature. In the Boosted Gaussian model the function $\phi_T(r,z)$ is given by

$$\phi_T(r,z) = N_T z(1-z)\exp\left(-\frac{m_f R^2}{8z(1-z)} - \frac{2z(1-z)r^2}{R^2} + \frac{m_f^2 R^2}{2}\right)\ . \tag{12}$$

In contrast, in the Gauss-LC model, it is given by

$$\phi_T(r,z) = N_T[z(1-z)]^2 \exp\left(-\frac{r^2}{2R_T^2}\right) \tag{13}$$

The parameters N_T, R and R_T are determined by the normalization condition of the wave function and by the decay width.

Lets initially present the main results for the J/Ψ production obtained in Ref. [22] using the Gaus-LC model and considering as input in our calculations the solution of the running coupling BK equation obtained in Ref. [79], denoting the corresponding predictions by rcBK hereafter. Moreover, we have considered phenomenological models which satisfy the asymptotic behaviours of the BK equation in order to fit the HERA and RHIC data (See e.g. Refs. [80, 81, 82, 72]). For comparison, in Ref. [22] we also have used the GBW model [80], which assumes that $\mathcal{N}_p(x,\boldsymbol{r},\boldsymbol{b}) = \mathcal{N}_p(x,\boldsymbol{r})S(\boldsymbol{b})$ with $\mathcal{N}_p(x,\boldsymbol{r}) = 1 - e^{-\boldsymbol{r}^2 Q_{s,p}^2(Y)/4}$ and $Q_{s,p}^2(Y) = (x_0/x)^\lambda$, with the parameters x_0 and λ determined by the fit to the HERA data. Moreover, we also have considered the b-CGC model proposed in Ref. [72], which improves the Iancu - Itakura - Munier (IIM) model [81] with the inclusion of the impact parameter dependence in the dipole - proton scattering amplitude. Following [72] we have:

$$\mathcal{N}_p(x,\boldsymbol{r},\boldsymbol{b}) = \begin{cases} \mathcal{N}_0 \left(\frac{r\,Q_{s,p}}{2}\right)^{2\left(\gamma_s + \frac{\ln(2/rQ_{s,p})}{\kappa\,\lambda\,Y}\right)} & rQ_{s,p} \leq 2 \\ 1 - \exp^{-A\,\ln^2(B\,r\,Q_{s,p})} & rQ_{s,p} > 2 \end{cases} \tag{14}$$

with $Y = \ln(1/x)$ and $\kappa = \chi''(\gamma_s)/\chi'(\gamma_s)$, where χ is the LO BFKL characteristic function. The coefficients A and B are determined uniquely from the condition that $\mathcal{N}_p(x,\boldsymbol{r},\boldsymbol{b})$, and its derivative with respect to rQ_s, are continuous at $rQ_s = 2$. In this model, the proton saturation scale $Q_{s,p}$ depends on the impact parameter:

$$Q_{s,p} \equiv Q_{s,p}(x,\boldsymbol{b}) = \left(\frac{x_0}{x}\right)^{\frac{\lambda}{2}} \left[\exp\left(-\frac{b^2}{2B_{\rm CGC}}\right)\right]^{\frac{1}{2\gamma_s}}. \tag{15}$$

The parameter $B_{\rm CGC}$ was adjusted to give a good description of the t-dependence of exclusive J/ψ photoproduction. The factors $\mathcal{N}_0$ and γ_s were taken to be free. In this way a very good description of F_2 data was obtained. One of the parameter set which is going to be used here is the one presented in the second line of Table II of [83]: $\gamma_s = 0.46$, $B_{CGC} = 7.5$ GeV^{-2}, $\mathcal{N}_0 = 0.558$, $x_0 = 1.84 \times 10^{-6}$ and $\lambda = 0.119$. More recently, the parameters of this model have been updated in Ref. [84] (considering the recently released high precision combined HERA data), becoming $\gamma_s = 0.6599$, $B_{CGC} = 5.5$ GeV^{-2}, $\mathcal{N}_0 = 0.3358$, $x_0 = 0.00105 \times 10^{-5}$ and $\lambda = 0.2063$. In Ref. [22] we have used these two sets of parameters in our calculations, with the resulting predictions being denoted bCGC and bCGC NEW, respectively. Moreover, in the case of coherent interactions in AA collisions we have calculated the cross sections considering that the nuclear scattering amplitude $N_A(x,r,b)$ is given by

$$N_A(x,r,b) = \left\{1 - \exp\left[-\frac{1}{2}AT_A(b)\,\sigma_{dip}(x,r)\right]\right\},$$

where $T_A(b)$ is the nuclear profile function, which will be obtained from a 3-parameter Fermi distribution for the nuclear density.

In Fig. 9 we present our predictions for the rapidity distribution for the diffractive photoproduction of J/Ψ in pp (left panel) and $PbPb$ (right panel) collisions. Due to the limitation

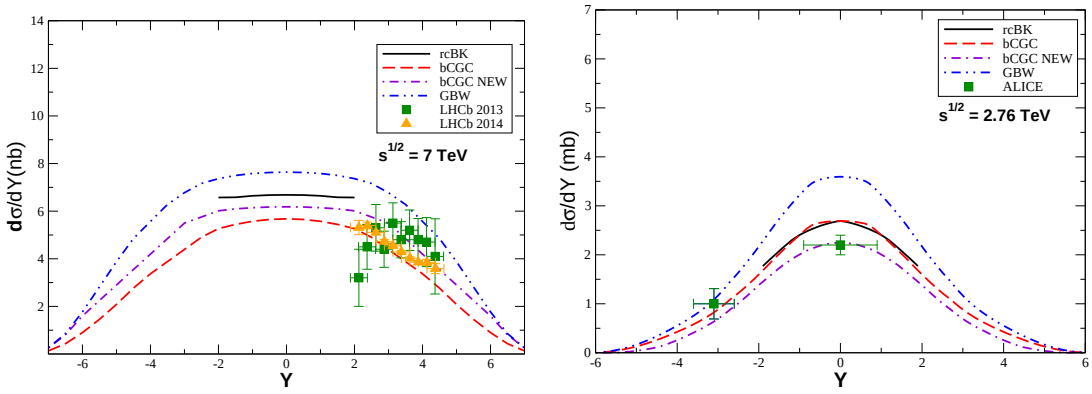

Figure 9. (Color online) Exclusive J/Ψ photoproduction in pp (left panel) and AA collisions (right panel) at the LHC. Data from LHCb [6, 7] and ALICE [4, 5] Collaborations.

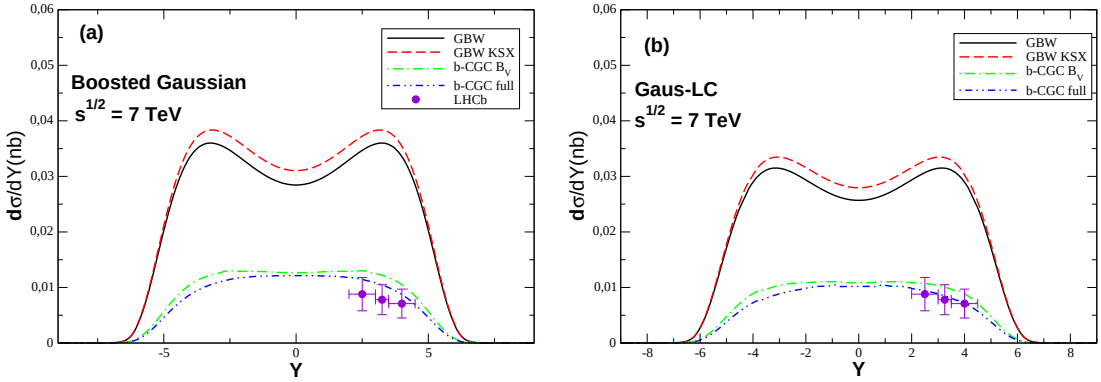

Figure 10. (Color online) Exclusive Υ photoproduction in pp collisions at $\sqrt{s} = 7$ TeV.

in the x-range of the rcBK solution, we were only able to present its predictions for a restricted rapidity range. In the case of pp collisions, we have obtained that the GBW (bCGC) prediction is an upper (lower) bound for the predictions at $Y = 0$. In particular, the predictions differ by ≈ 30 % for central rapidities at $\sqrt{s} = 7$ TeV. For the rapidity range probed by the LHCb Collaboration the difference is larger (≈ 50 %). We obtain that the bCGC and bCGC NEW predictions agree with the data from LHCb Collaboration [6, 7]. These differences increase with the energy, which motivates future experimental analysis of this process in order to constrain the dipole - proton scattering amplitude and, consequently, the QCD dynamics at high energies. In the case of the J/Ψ in $PbPb$ collisions, we obtain that the distinct predictions largely differ at central rapidities. We have obtained that the bCGC NEW prediction is able to describe the current ALICE data [4, 5], in contrast with the other predictions which overestimate the data for $Y = 0$. In particular, the rcBK prediction is not able to describe the data, in agreement with the results obtained in Ref. [20]. As demonstrated in Ref. [22], the difference between the predictions is amplified at larger energies. The main conclusion in Ref. [22] was that the color dipole formalism is able to describe current data for the J/Ψ production and that future measurements can be useful to constrain the magnitude of the non linear effects in the QCD dynamics.

In Ref. [23] we have extended our studies of vector meson production in hadronic collisions for the case of the Υ production. In particular, we have compared the predictions obtained using the Boosted Gaussian and Gaus-LC models for the vector meson wave function, as well as

the different ways to estimate the total cross section described in Eqs. (9) and (10). Moreover, we have considered an updated version of the GBW model, obtained in Ref. [85] considering the ZEUS data available in 2007 (denoted GBW-KSX hereafter). It is important to emphasize that the GBW model is a model for the forward dipole-target amplitude $\mathcal{N}_p(x, \boldsymbol{r})$, which does not allow us to calculate the t-dependence of the differential cross section. Therefore, in the GBW case, we should estimate the total cross section using Eq. (10). In Fig. 10 we present our predictions for the rapidity distribution of exclusive Υ photoproduction in pp collisions at $\sqrt{s} = 7$ TeV. It is important to emphasize that the bCGC predictions were obtained using the updated version of this model, denoted bCGC NEW in the plots for the J/Ψ production. The Boosted Gaussian and Gauss-LC predictions are presented in the panels (a) and (b), respectively. We obtain that the GBW-KSX (bCGC full) prediction is an upper (lower) bound for the predictions at $Y = 0$. We have obtained that the bCGC full and B_V predictions are almost identical at central rapidities and differ by ≈ 10 % for $Y = 4$. The GBW-KSX and GBW predictions differ by ≈ 10 % in the $|Y| \leq 4$ range. In contrast, the GBW and bCGC predictions differ by a factor 2.7 (3.5) at $Y = 0\,(4)$. The Boosted Gaussian predictions are larger than the Gauss-LC one, with the difference being of ≈ 12 % at $Y = 0$. It important to emphasize that the predictions presented in Ref. [23] were obtained before the publication of the experimental data by the LHCb Collaboration [8]. The Fig. 10 is an updated version of the figure presented in [23] including these data, which demonstrate that they agree very well with the bCGC predictions, which also describe the J/Ψ data.

4. Probing the Odderon at the LHC

Understanding the behaviour of high energy hadron reactions from a fundamental perspective within of Quantum Chromodynamics (QCD) is an important goal of particle physics (For recent reviews see e.g. Ref. [35]). The central papers concerning the knowledge of the Regge limit (high energy limit) of perturbative QCD (pQCD) were presented in the mid seventies by Lipatov and collaborators [86], which demonstrated that the high energy behaviour of the total cross sections is related to the Pomeron exchange. In the framework of perturbative QCD the Pomeron corresponds to a C-even parity (C being the charge conjugation) compound state of two t-channel reggeized gluons, given by the solution of the Balitsky - Fadin - Kuraev - Lipatov (BFKL) equation [86]. Besides the Pomeron, a natural prediction of the QCD is the presence of the so-called Odderon, which is a C-odd compound state of three reggeized gluons, which dominates the hadronic cross section difference between the direct and crossed channel processes at very high energies. The Odderon is described by the Bartels - Kwiecinski - Praszalowicz (BKP) equation [87], which resums terms of the order $\alpha_s(\alpha_s \log s)^n$ with arbitrary n in which three gluons in a $C = -1$ state are exchanged in the t-channel.

In the last years, the physics of the Odderon has become an increasingly active subject of research, both from theoretical and experimental points of view (For a recent review see [88]). On the theoretical side, the investigation of the Odderon in pQCD has led to discovery of relations of high energy QCD to the theory of integrable models [89] and two leading solutions of the BKP evolution equation were obtained [90, 91], with the intercept being close to or exactly one, depending on the scattering process. In contrast, on the experimental side, the existence of the Odderon is still not confirmed, with the experimental evidence for the Odderon being at the moment rather scarce. An alternative to probe the Odderon is the study of the diffractive photoproduction of pseudoscalar mesons in ep collisions. As the real photon emitted by the electron carries negative C parity, its transformation into a diffractive final state system of positive C parity requires the t-channel exchange of an object of negative C parity. It implies that Pomeron exchange cannot contribute to this process and that it can only be mediated by the exchange of an Odderon. A particular promising process is the diffractive η_c photoproduction, since the meson mass provides a hard scale that makes a perturbative calculation possible

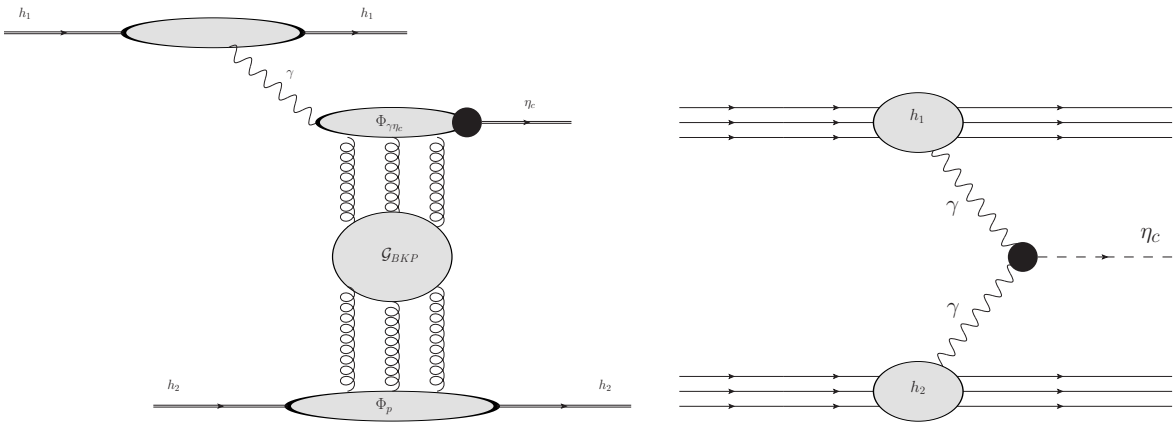

Figure 11. (Color online) η_c production in photon - hadron (left panel) and photon - photon (right panel) interactions.

[93, 92]. Unfortunately, even with an optimistic choice of the strong running coupling constant α_s, the cross section for this process was too small to be observed at HERA. Consequently, the current experimental evidence for the Odderon is very unsatisfactory.

In Ref. [28] we proposed the study of coherent hadron - hadrons interactions as a new alternative to search the Odderon in high energy pp and AA collisions at CERN - LHC. Recently, this study was extended for the kinematical range probed by the AFTER@LHC experiment in Ref. [29]. As discussed in the Introduction, the basic idea in coherent hadronic collisions is that the total cross section for a given process can be factorized in terms of the equivalent flux of photons into the hadron projectile and the photon-photon or photon-target production cross section. Consequently, coherent interactions can be used to study the diffractive η_c photoproduction, which is a direct probe of the Odderon. In Fig. 11 (left panel) we present an illustration of the coherent process $h_1 + h_2 \to h_1 h_2 \eta_c$. It is important to emphasize that the η_c can also be produced in photon - photon ($\gamma\gamma$) interactions as illustrated in Fig. 11 (right panel), with both processes generating two rapidity gaps in the final state. While the η_c production in γh interactions is a direct probe of the Odderon, its production in $\gamma\gamma$ interactions is an important background, which should be estimated in order to separate the signal associated to the Odderon. In what follows we present a brief review of the main results from Refs. [28, 29].

The cross section for the diffractive η_c photoproduction can be obtained using the impact factor representation, proposed by Cheng and Wu [94] many years ago. In this representation, the amplitude for a large-s hard collision process can be factorized in three parts: the two impact factors of the colliding particles and the Green's function for the three interacting reggeized gluons, which is determined by the BKP equation and is represented by $\mathcal{G}_{\rm BKP}$ hereafter. The differential cross section for the process $\gamma + h \to \eta_c + h$ is given by [92]

$$\frac{d\sigma}{dt} = \frac{1}{32\pi} \sum_{i=1,2} |\mathcal{A}^i|^2 \; , \tag{16}$$

where $\mathcal{A}^i$ is the amplitude for a given transverse polarization i of the photon, which can be expressed as a convolution of the impact factors for the proton (Φ_p) and for the $\gamma\eta_c$ transition ($\Phi^i_{\gamma\eta_c}$) with the Odderon Green function:

$$\mathcal{A}^i = \frac{5}{1152} \frac{1}{(2\pi)^8} \langle \Phi^i_{\gamma\eta_c} | \mathcal{G}_{BKP} | \Phi_p \rangle \; . \tag{17}$$

Differently from $\Phi^i_{\gamma\eta_c}$, that can be calculated perturbatively [93], the impact factor Φ_p that describes the coupling of the Odderon to the proton is non-perturbative and should be modelled. In our calculations we consider the model used in Refs. [93, 92] (We refer the reader to the original papers for the details). The Odderon Green function $\mathcal{G}_{BKP}$ is described in terms of the solution of the BKP equation [87], with the energy dependence being determined by the Odderon intercept $\alpha_{I\!O}$. Currently, two leading solutions of the Odderon evolution equations are available [90, 91] and the subject continues to be under intensive study. In Ref. [90], Janik and Wosiek (JW) obtained that $\alpha_{I\!O} = 1 - 0.24717\frac{\alpha_s N_c}{\pi}$, which for $\alpha_s \approx 0.2$ yields $\alpha_{I\!O} = 0.96$. Moreover, they found that its solution does not couple to all phenomenologically relevant impact factors. In particular, the coupling for the $\gamma\eta_c$ impact factor vanishes in leading order. In contrast, Bartels, Lipatov and Vacca (BLV) [91] have found a solution for the BKP equation with intercept $\alpha_{I\!O}$ exactly equal to one and that couples to $\Phi_{\gamma\eta_c}$, in contrast to the JW solution. Such solution was used in [92] to estimate the diffractive η_c photoproduction in the kinematical region probed in ep collisions at HERA (BBCV model hereafter). They find a weak logarithmic suppression with the energy and have predicted an integrated cross section of ≈ 50 pb at HERA energy. This prediction is a factor 5 larger than the value obtained by Kwiecinski and collaborators in Ref. [93] (CKMS model hereafter), which has considered a simplified three gluon exchange model for the Odderon that implies an energy independent cross section. A shortcoming of these analysis is the large value used for the effective strong coupling constant present in the coupling of the Odderon to the external particles. As pointed in Ref. [95] the cross sections reported in Refs. [92, 93] have to be reduced by a factor 30. In Refs. [28, 29] we have considered the approach proposed in Ref. [92] and used a more realistic value for α_s ($= 0.3$). For completeness we also have presented the results of the approach proposed in [93].

In Table 2 we present our predictions for the total cross section considering pp collisions at $\sqrt{s_{NN}} = 8$ and 14 TeV. We predict values of the order of pb, with the BBVC prediction being a factor of ≈ 20 larger than the CKMS one. This large factor of enhancement is directly associated to the energy dependence present in the BBVC model, which implies that the γh cross section increases at smaller energies, while the CKMS predicts an energy independent cross section. It is important to emphasize that the main contribution for the total $h_1 h_2$ cross section comes from small values of ω due to dependence of the equivalent photon spectrum in the photon energy, which is proportional to $1/\omega$. Furthermore, the increasing of the photon flux with $\sqrt{s_{NN}}$ implies that $\sigma(h_1 h_2 \to h_1 \otimes \eta_c \otimes h_2)$ also increases with the center-of-mass energy. In comparison to the cross sections for the J/Ψ photoproduction [18], our predictions are a factor $\geq 10^3$ smaller, with the difference increasing with the energy due to the Pomeron exchange present in the J/Ψ production. In Table 3 we present our predictions for the total cross section considering $PbPb$ collisions at two values of center-of-mass energy. As the photon flux is proportional to Z^2, because the electromagnetic field surrounding the ion is very larger than the proton one due to the coherent action of all protons in the nucleus, the nuclear cross sections are amplified by this factor. Moreover, our predictions also are amplified by the mass number A, since in our calculations for the nuclear case we have assumed in a first approximation that $\sigma(\gamma A \to \eta_c A) = A.\sigma(\gamma p \to \eta_c p)$. Consequently, we predict cross sections of the order of μb for the diffractive η_c photoproduction in $PbPb$ collisions at LHC. Considering the design luminosities at LHC for pp collisions ($\mathcal{L}_{\rm pp} = 10^{34}$ cm^{-2}s^{-1}) and $PbPb$ collisions ($\mathcal{L}_{\rm PbPb} = 4.2 \times 10^{26}$ cm^{-2}s^{-1}) we have calculated the production rates (See Tables 2 and 3). Although the cross section for the diffractive η_c photoproduction in AA collisions is much larger than in pp collisions, the event rates are higher in the pp mode due to its larger luminosity. In particular, we predict that the events rate/year for pp collisions at $\sqrt{s} = 14$ TeV should be larger than 65000.

In Table 4 we present our predictions for the total cross sections in the kinematical range probed by the AFTER@LHC experiment [96]. We predict cross sections for the η_c production in Pbp and $PbPb$ collisions that are a factor $\geq 10^4$ larger than the pp predictions. For the

$\sqrt{s_{NN}}$	CKMS	BBCV
8 TeV	$0.55\,pb$ (55000)	$10.10\,pb$ (1×10^6)
14 TeV	$0.65\,pb$ (65000)	$13.90\,pb$ (1.4×10^6)

Table 2. Cross sections (event rates/year) for the diffractive η_c photoproduction in pp collisions at LHC energies.

$\sqrt{s_{NN}}$	CKMS	BBCV
2.76 TeV	$0.30\,\mu b$ (126)	$14.25\,\mu b$ (5985)
5.5 TeV	$0.40\,\mu b$ (168)	$23.59\,\mu b$ (9912)

Table 3. Cross sections (event rates/year) for the diffractive η_c photoproduction in $PbPb$ collisions at LHC energies.

h_1h_2	CKMS	BBCV
pp ($\sqrt{s}=115$ GeV)	0.05 pb (1000.0)	0.30 pb (6000.0)
Pbp ($\sqrt{s}=72$ GeV)	28.1 pb (31.0)	356.6 pb (393.0)
$PbPb$ ($\sqrt{s}=72$ GeV)	5870.0 pb (41.0)	74366.0 pb (520.0)

Table 4. Cross sections (event rates/year) for the exclusive η_c photoproduction in $pp/Pbp/PbPb$ collisions at AFTER@LHC experiment.

exclusive η_c production in pp collisions we predict values of the order of a fraction of pb, with the BBVC prediction being a factor of ≈ 6 larger than the CKMS one. This enhancement is directly associated to the energy dependence present in the BBVC model, which implies that the γh cross section increases at smaller energies, while the CKMS predicts an energy independent cross section. For the η_c production in Pbp and $PbPb$ collisions, we predict cross sections of the order of nb for the exclusive η_c photoproduction in $PbPb$ collisions at AFTER@LHC experiment. Moreover, we predict that the Pbp cross sections are two orders of magnitude smaller than those predicted for $PbPb$ collisions. In Ref. [29] we have estimated the background associated to the η_c production in $\gamma\gamma$ interactions for pp collisions and obtained that $\sigma[pp \stackrel{(\gamma\gamma)}{\longrightarrow} p\otimes\eta_c\otimes p] = 2.2$ pb, which is a factor ≈ 8 larger than the predictions for the η_c production in photon - hadron interactions. As both processes generate two rapidity gaps in the final state, the detection of the gaps is not, in a first analysis, an efficient trigger for the separation of the γh production of the η_c. An alternative is the reconstruction of the entire event with a cut on the summed transverse momentum of the event. As the typical photon virtualities are very small, the hadron scattering angles are very low. Consequently, we expect that a different transverse momentum distribution of the scattered hadron, with γh interactions predicting larger p_T values. In contrast, the background is not present in nuclear collisions, since the maximum $\gamma\gamma$ center-of-mass energies in Pbp and $PbPb$ collisions are smaller than threshold of production. Considering the design luminosities at AFTER@LHC for pp ($\mathcal{L}_{\rm pp} = 2\times10^4$ pb^{-1}yr^{-1}), Pbp ($\mathcal{L}_{\rm Pbp} = 1.1$ pb^{-1}yr^{-1}) and $PbPb$ collisions ($\mathcal{L}_{\rm PbPb} = 7.0\times10^{-3}$ pb^{-1}yr^{-1}) we can calculate the production rates (See Table 4). Although the cross section for the exclusive η_c photoproduction in $PbPb$ collisions is much larger than in pp collisions, the event rates are higher in the pp mode due to its larger luminosity. In particular, we predict that the events rate/year for pp collisions at $\sqrt{s} = 115$ GeV should be larger than 1000. On the other hand, for Pbp and $PbPb$ collisions at $\sqrt{s} = 72$ GeV we predict that the events rate/year should be larger than 30. Although smaller than the

pp predictions, the observation of the η_c production in nuclear collisions would clearly indicate the existence of the Odderon.

5. Probing Charmoniumlike exotic states at the LHC

In the past eleven years a series of charmoniumlike states X, Y, Z has been announced at various experimental facilities (For recent reviews see, *e.g.*, Refs. [97, 98, 99]). These exotic mesons are a class of hadrons that decay to final states that contain a heavy quark and a heavy antiquark but cannot be easily accommodated in the remaining unfilled states in the $c\bar{c}$ level scheme. One of the most interesting exotic states are the charged states, *e.g.* $Z(4430)$ and $Z_c(3900)$, that clearly have a more complex structure than $c\bar{c}$ pair, being natural candidates for molecular or tetraquarks states.

So far, most of the available experimental and theoretical investigations of the charmoniumlike exotic candidates have been focused on the spectrum and decays or the production in e^+e^- collisions. In order to decipher the nature of these states, more accurate data and new processes involving these states would be equally important. The search of X, Y, Z charmoniumlike states by other production processes will not only confirm these observed states, but also will be useful to study their underlying structures. In the last years, the study of the production of exotic hadrons in proton - proton [100], heavy ion [101] and photon - hadron [102, 103, 104, 105] collisions was proposed by several authors. In particular, the results obtained in Refs. [102, 104] for the photoproduction of charged charmoniumlike states $Z(4430)$ and $Z_c(3900)$ indicate a large enhancement of the cross section near the threshold, which could be considered a signature for the existence of these states in γp collisions. Unfortunately, as the DESY - HERA ep collider stopped its operations in 2007, the experimental analysis of these states in photon - hadron collisions was not possible and remains an open question.

The production of some exotic states in $\gamma\gamma$ interactions considering pp collisions at LHC energies was analysed in Ref. [106], which have demonstrated that the experimental analysis of these states is, in principle, feasible. A similar conclusion was obtained in Ref. [107] for $PbPb$ collisions. On the other hand, in Ref. [108] we have proposed by the first time the study of the charmoniumlike exotic states in γp interactions at the RHIC and LHC and demonstrated that this process provide complementary and independent checks on the properties of the exotic states, and help to understand their underlying nature. In particular, in Ref. [108] we estimated the photoproduction of the charmoniumlike states $Y(3940)$, $X(3915)$, $Z(4430)$ and $Z_c(3900)$ in proton - proton collisions at the RHIC and LHC and shown that the prospect to observe these states is rather promising and thus an experimental analysis is strongly motivated. In this Section we will briefly review our results for the $Z_c(3900)$ photoproduction since the results for the other exotic states can be obtained in a similar way (For details see Ref. [108]).

The main input in our calculations is the photon - hadron cross section for the production of the of exotic charmoniumlike state $\sigma_{\gamma p \to H_c}$. Currently the unique available predictions in the literature [102, 103, 104, 105] were obtained considering an effective Lagrangian approach combined with the vector meson dominance (VMD) assumption [109]. In this approach the interaction is described in terms of a meson exchange, which is neutral/charged for the production of neutral/charged exotic charmoniumlike states. Considering the approach proposed in Ref. [104] the photoproduction of the $Z_c(3900)^+$ in pp collisions is described by the diagram presented in Fig. 12(a), where we also represent the decay of the exotic meson in a $J/\Psi + \pi^+$ final state, which we assume to be the dominant channel. The basic idea is that the photon stemming from the electromagnetic field of one of the incident protons fluctuates into a J/Ψ which interacts with the other proton through the π^+ exchange producing a neutron n and a $Z_c(3900)^+$ state which decays in the $J/\Psi + \pi^+$ system. Assuming the VMD model to describe the coupling between the intermediate vector meson and the photon, an effective Lagrangian to describe the coupling between the pion and the nucleons and another describing the $Z_c J/\Psi \pi$

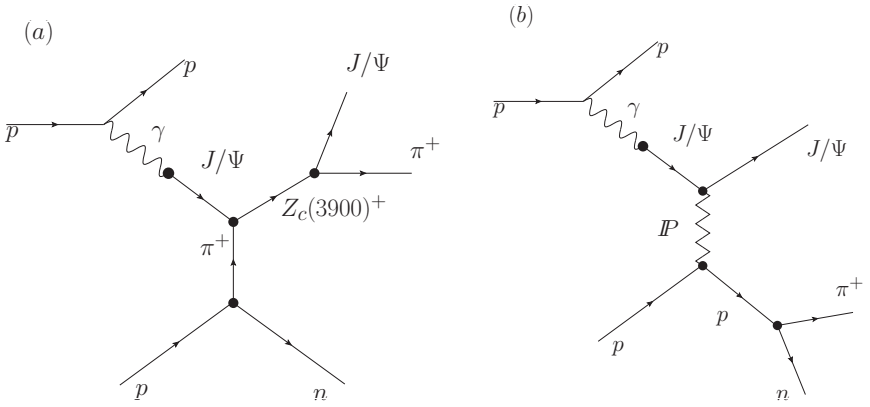

Figure 12. (a) The $pp \to pZ_c^+ n \to pJ/\Psi\pi^+ n$ process through the π^+ exchange. (b) The $pp \to pJ/\Psi\pi^+ n$ process through the Pomeron exchange.

coupling, the squared amplitude for the process $\gamma p \to Z_c^+ n$ can be expressed by (See Ref. [104] for details)

$$|\mathcal{M}|^2 = \mathcal{C}\frac{-q^2(q^2 - M_{Z_c}^2)^2}{(q^2 - m_\pi^2)^2} F_{\pi NN}^2 F_{Z_c J/\Psi\pi}^2 \tag{18}$$

where q is the four momentum of the pion exchanged and

$$\mathcal{C} = \left(\sqrt{2} g_{\pi NN} \frac{g_{Z_c J/\Psi\pi}}{M_{Z_c}} \frac{e}{f_{J/\Psi}}\right)^2 \tag{19}$$

with the couplings $g_{\pi NN}$, $e/f_{J/\Psi}$ and $g_{Z_c J/\Psi\pi}$ being respectively determined assuming that $g_{\pi NN}^2/4\pi = 14$, by the decay $J/\Psi \to e^+e^-$ and by the decay width of $Z_c \to J/\Psi\pi$. In what follows we assume $\Gamma[Z^+ \to J/\Psi\pi^+] = 29$ MeV as calculated in [110]. Moreover, the form factors $F_{\pi NN}$ and $F_{Z_c J/\Psi\pi}$ are given by

$$F_{\pi NN} = \left(\frac{\Lambda_\pi^2 - m_\pi^2}{\Lambda_\pi^2 - q^2}\right), \quad F_{Z_c J/\Psi\pi} = \left(\frac{\Lambda_{Z_c}^2 - m_\pi^2}{\Lambda_{Z_c}^2 - q^2}\right) \tag{20}$$

where we assume $\Lambda_\pi = 0.7$ GeV and $\Lambda_{Z_c} = M_{J/\Psi}$ for the cut-offs. The resulting γp cross section is strongly enhanced close to the threshold [104]. This formalism can be directly extended to take into account the Z_c decay in the $J/\Psi + \pi$ final state. However, as this final state can also be produced in a γp interaction through the Pomeron exchange, we should include this background in our calculations. In Fig. 12(b) we present a typical diagram for the background contribution. Following Ref. [111] we assume that the Pomeron behaves like an isoscalar photon with $C = +1$. The corresponding amplitude has a Regge-like energy dependence $\propto s^{\alpha_{I\!P}(t)-1}$, where $\alpha_{I\!P}(t) = 1 + \Delta + \alpha' t$ is the Pomeron trajectory, Δ is the Pomeron intercept, $\alpha' = 0.25$ GeV^{-2} and t is the exchanged Pomeron momentum squared.

In Fig. 13 we present our predictions for the rapidity distribution for the production of a $J/\Psi + \pi$ final state in pp collisions at RHIC ($\sqrt{s} = 0.2$ TeV) and LHC ($\sqrt{s} = 14$ TeV) energies considering the diagrams presented in Figs. 12 (a) and (b). The cross section for the background, associated to the Pomeron exchange, has been estimated considering two different values for the Pomeron intercept $\Delta = 0$ and 0.08, which determines its energy dependence. At RHIC energy

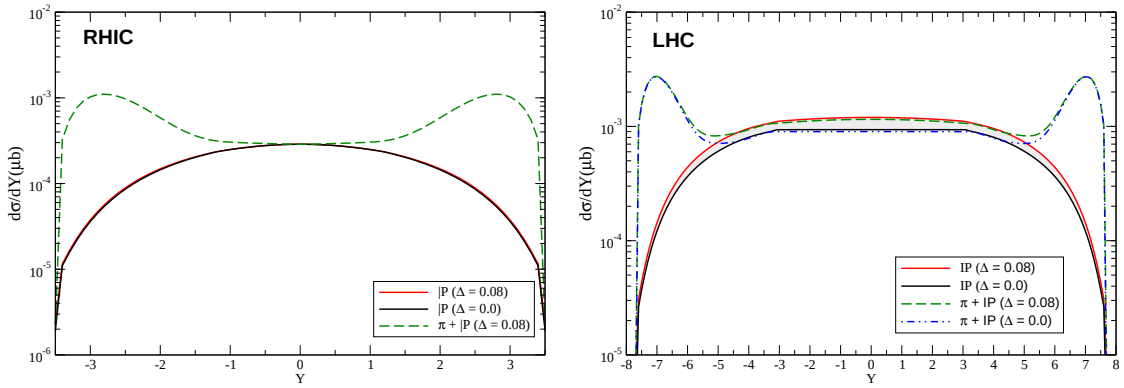

Figure 13. (Color online) Rapidity distribution for the photoproduction of a $J/\Psi + \pi$ final state in pp collisions at RHIC ($\sqrt{s} = 0.2$ TeV) and LHC ($\sqrt{s} = 14$ TeV) energies. The solid lines represent the background associated to the Pomeron exchange for two values of the intercept Δ. The dashed lines represent the sum of the background with the signal associated to the $\gamma p \to Z_c(3900)^+ n \to J/\Psi \pi n$ interaction through π exchange.

these two predictions for the Pomeron contribution are almost identical, while at LHC they differ by almost 10 % at $Y = 0$. We predict that the signal dominates the rapidity distributions for large values of the rapidity $|Y|$, where we are probing the γp cross section at small values of the c.m. energy. The resonancelike structure present in the γp cross section, which is a signature of the Z_c^+ production, can be directly probed at $|Y| \geq 2.0\,(5.5)$ at RHIC (LHC) energy. A similar behaviour is predicted in the rapidity distribution for the photoproduction of the $Z(4430)^+$. These results shown that the resulting cross sections for the $Z_c(3900)$ photoproduction at the RHIC energy are at 1 nb level, while at LHC are larger by roughly one order of magnitude. Taking into account the design luminosity at the LHC the number of events has been estimated, being of the order of 10 events/second for this processes. The results presented in Ref. [108] indicated that the four exotic states analysed could be copiously produced. Consequently, we believe that the study of these states at RHIC and LHC is feasible and will provide valuable information on hadron spectroscopy as well as hadron interactions.

6. Probing the Photon Flux at the LHC

The equivalent photon approximation of a charged pointlike fermion was formulated many years ago by Fermi [112] and developed by Williams [113] and Weizsacker [114]. In contrast, the calculation of the photon distribution of the hadrons still is a subject of debate, due to the fact that they are not point like particles. In this case it is necessary to distinguish between the elastic and inelastic components (See Fig. 14). The elastic component [Fig. 14 (a)] can be estimated analysing the transition $h \to \gamma h$ taking into account the effects of the hadronic form factors, with the hadron remaining intact in the final state [115]. In contrast, the inelastic contribution [Fig. 14 (b)] is associated to the transition $h \to \gamma X$, with $X \neq h$, and can be estimated taking into account the partonic structure of the hadrons, which can be a source of photons (See, e.g. Refs. [34, 116, 117, 118, 119, 120, 121, 122]). Therefore the total photon distribution of a hadron is given by

$$\gamma(x, \mu^2) = \gamma_{el}(x) + \gamma_{inel}(x, \mu^2) \tag{21}$$

where x is the fraction of the hadron energy carried by the photon and μ has to be identified with a momentum scale of the photon - induced process. It is important to emphasize that

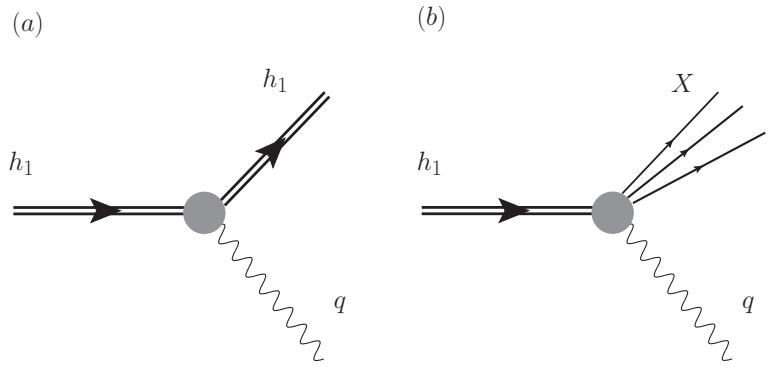

Figure 14. (a) Elastic and (b) Inelastic components of the equivalent photon distributions of a hadron.

while γ_{el} is proportional to squared charge of the hadron (Z^2), due to the coherent action of all protons in the nucleus, γ_{inel} is proportional to the mass number A. Consequently, for a heavy nuclei, the total photon distribution is determined by its elastic component. In contrast, for a proton, both components contribute equally and should be taking into account in the study of photon - induced processes. Currently, the description of the inelastic component still is an open question, with the predictions for its x dependence being largely distinct.

The concept of the photon content of a charged fermion is based on the equivalent photon approximation (EPA) [34, 33], which implies that the photon distribution of a nucleon consist of two parts: the elastic and inelastic components. A detailed derivation of the elastic photon distribution of a nucleon was presented in Ref. [115] which can be written as

$$\gamma_{el}(x) = -\frac{\alpha}{2\pi}\int_{-\infty}^{-\frac{m^2x^2}{1-x}} \frac{dt}{t}\left\{\left[2\left(\frac{1}{x}-1\right)+\frac{2m^2x}{t}\right]H_1(t)+xG_M^2(t)\right\}\ , \tag{22}$$

where $t = q^2$ is the momentum transfer squared of the photon,

$$H_1(t) \equiv \frac{G_E^2(t)+\tau G_M^2(t)}{1+\tau} \tag{23}$$

with $\tau \equiv -t/m^2$, m being the nucleon mass, and where G_E and G_M are the Sachs elastic form factors. Although an analytical expression for the elastic component is presented in Ref. [115], it is common to found in the literature the study of photon - induced processes considering an approximated expression proposed in Ref. [123], which can be obtained from Eq. (22) by disregarding the contribution of the magnetic dipole moment and the corresponding magnetic form factor. As demonstrated in Ref. [106] the difference between the full and the approximated expression is smaller than 5% at low-x. Consequently, in what follows we will use the expression proposed in Ref. [123], where the elastic photon distribution is given by

$$\gamma_{el}(x) \;=\; \frac{\alpha}{\pi}\left(\frac{1-x+0.5x^2}{x}\right)\times\left[\ln(\Omega)-\frac{11}{6}+\frac{3}{\Omega}-\frac{3}{2\Omega^2}+\frac{1}{3\Omega^3}\right]\ , \tag{24}$$

where $\Omega = 1+(0.71\mathrm{GeV}^2)/Q^2_{min}$ and $Q^2_{min} \approx (xm)^2/(1-x)$.

On the other hand, there are different models for the contribution of the inelastic component of the photon distribution of a nucleon. In Ref. [117], a naive approach to the photon flux

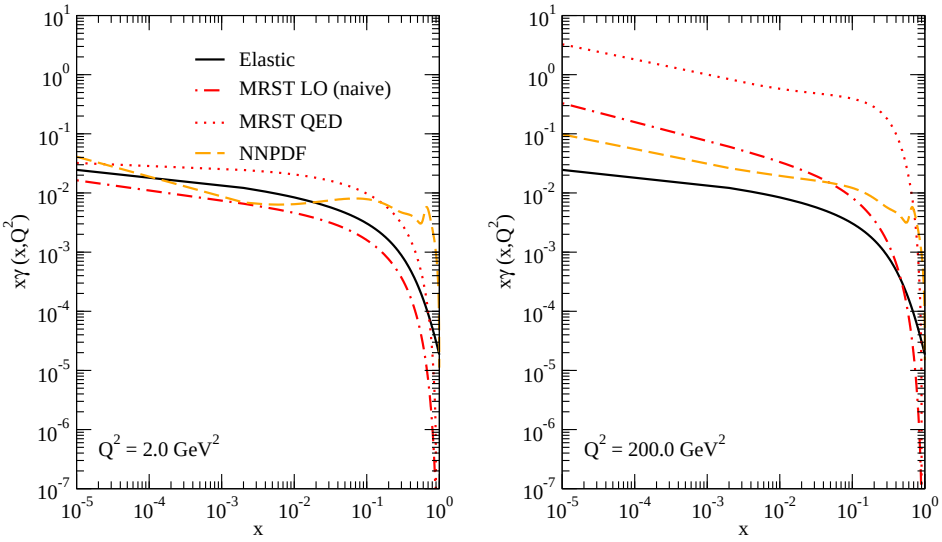

Figure 15. (Color online) Comparison between the different models for the inelastic photon distribution for two different values of the hard scale $\mu^2 = Q^2$. The elastic component is presented for comparison.

was proposed, with the photon distribution in the proton being given by a convolution of the distribution of quarks in the proton and the distribution of photons in the quarks as follows

$$\gamma_{inel}(x,\mu^2) = \sum_q \int_x^1 \frac{dx_q}{x_q} f_q(x_q,\mu^2) e_q^2 f_{\gamma/q}(\frac{x}{x_q}, Q_1^2, Q_2^2) \ , \tag{25}$$

where the sum runs over all quark and antiquark flavours and the flux of photons in a quark $f_{\gamma/q}$ is given by

$$f_{\gamma/q}(z) = \frac{\alpha}{2\pi} \frac{1+(1-z)^2}{z} \log \frac{Q_1^2}{Q_2^2} \ , \tag{26}$$

with Q_1^2 being assumed to be the maximum value of the momentum transfer in the process and Q_2^2 is assumed to be equal to 1 GeV^2 in order to the parton model to be applicable. Recently, different groups have studied the modification of the Dokshitzer - Gribov - Lipatov - Altarelli - Parisi equations for the quark and gluon distributions by the inclusion of QED contributions and have performed global parton analysis of deep inelastic and related hard-scattering data [119, 120, 121, 122]. Basically, the DGLAP equations and the momentum sum rule are modified considering the presence of the photon as an additional point-like parton in the nucleon. The parametrizations for the photon distribution currently available in the literature [119, 120] differ in the approach for the initial condition for the photon distribution. While the MRST group assume that $\gamma_{inel}(x,Q_0^2)$ is given by a expression similar to Eq. (25), the NNPDF group parametrize the input photon PDF and attempt to determine the parameters from the global data. The preliminary CTEQ analysis presented in Ref. [121] assume a similar theoretical form for $\gamma_{inel}(x,Q_0^2)$ to that proposed by the MRST group, but with an arbitrary normalization parameter, which is expressed as the momentum fraction carried by the photon. More recently, a distinct approach for the initial condition for the evolution of the photon distribution was proposed in Ref. [122], where the authors have proposed that the starting distribution for the photon PDF should be the total photon distribution, i.e. by the sum of the

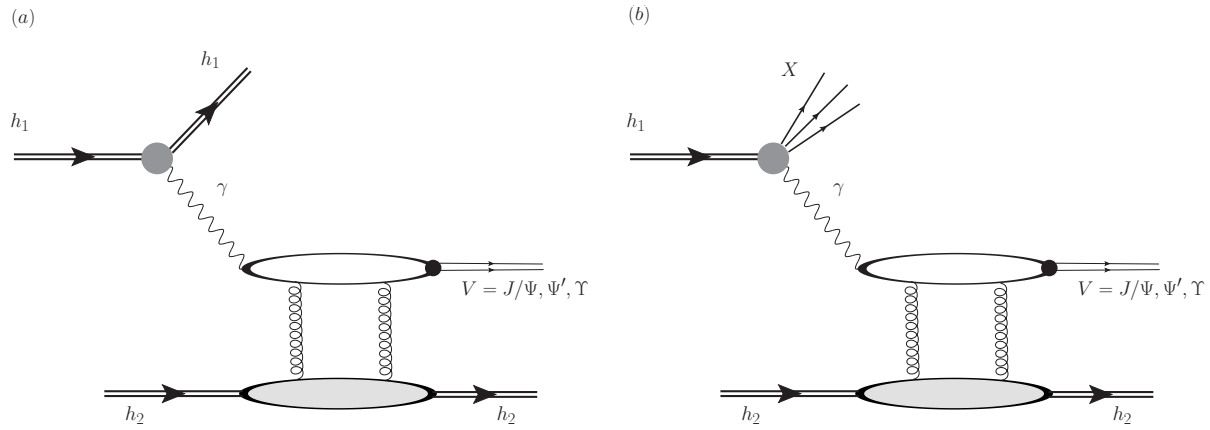

Figure 16. Diffractive quarkonium photoproduction in hadronic collisions associated to the (a) elastic and (b) inelastic component of the photon distribution of the hadron.

elastic and inelastic components as given in Eq. (21). The main motivation of this approach is the reduced uncertainty in the input photon PDF, since the major part of the distribution is given by the elastic component, which is well known. As a consequence of this assumption, the elastic component is dominant also at large values of the hard scale μ^2 (See Fig. 5 in [122]). Unfortunately, the current data is not sufficient accurate to precisely determine the initial condition. Thus the current predictions for the inelastic photon component strongly differ in its x dependence. In what follows we will consider the MRST2004QED and NNPDF parametrizations, since only these two are currently available to public use. In Fig. 15 we present the predictions of the MRST2004QED and NNPDF parametrizations for the inelastic photon distribution considering two different values for the hard scale μ^2. For comparison the predictions of the Naive approach [Eq. (25)] and the elastic component [Eq. (24)] are also presented. While the elastic component is independent of the hard scale μ^2, the inelastic component is strongly dependent, increasing at larger values of μ^2. Moreover, all models predict that the inelastic contribution is dominant at very small values of x. However, as demonstrated in the figure, the x-dependence of the inelastic parametrizations is very distinct. This result motivates the analysis of observables which are strongly dependent on the photon flux.

In Refs. [30, 31] we have proposed to probe the photon flux of a proton in the analysis of two different processes at the LHC: (a) in the diffractive vector meson photoproduction and (b) in the dilepton and W^+W^- production in two - photon interactions. Lets initially present the basic concepts and main results from Ref. [30]. As discussed before, the diffractive vector meson production in ultra peripheral heavy ion collisions (UPHIC) have been largely discussed in the literature in the last years [129, 12, 13, 14, 132, 16, 17, 131, 24, 18, 13, 19, 20, 21, 15, 22, 23]. However, such studies have only considered the process in which the hadron which emits the photon remain intact represented in Fig. 16 (left panel). In other words, these studies have assumed that the total photon distribution is dominated by the elastic component and that the hadron which emits the photon remains intact. Such approximation is reasonable for a nuclear projectile. On the other hand, for a proton projectile, the magnitude of the contribution associated to the inelastic component of the photon distribution, where the proton which emits the photon dissociates, represented in Fig. 16 (right panel), was an open question, discussed by the first time in Ref. [30]. In Ref. [30] we have estimate the diffractive vector meson production

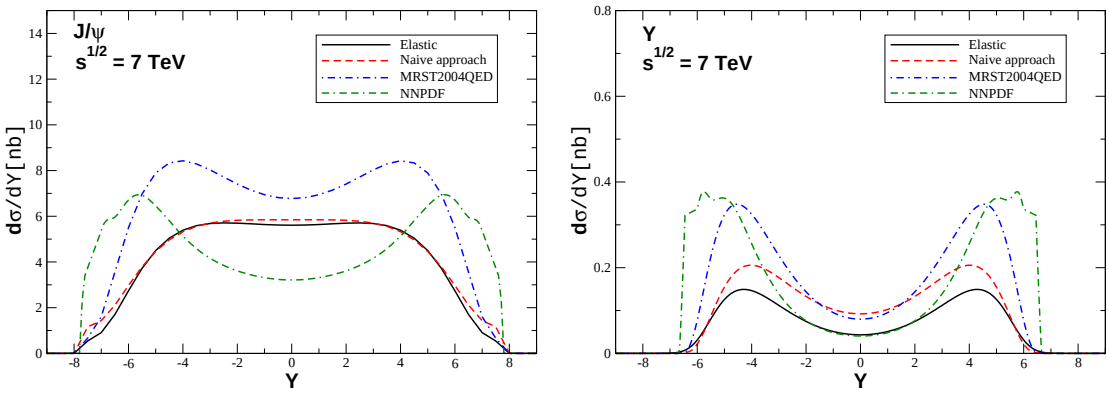

Figure 17. (Color online) Rapidity distribution for the diffractive J/Ψ and Υ photoproduction in pp collisions at LHC ($\sqrt{s} = 7$ TeV) considering different models for the inelastic component of the photon distribution. The predictions associated to the elastic component are also presented for comparison.

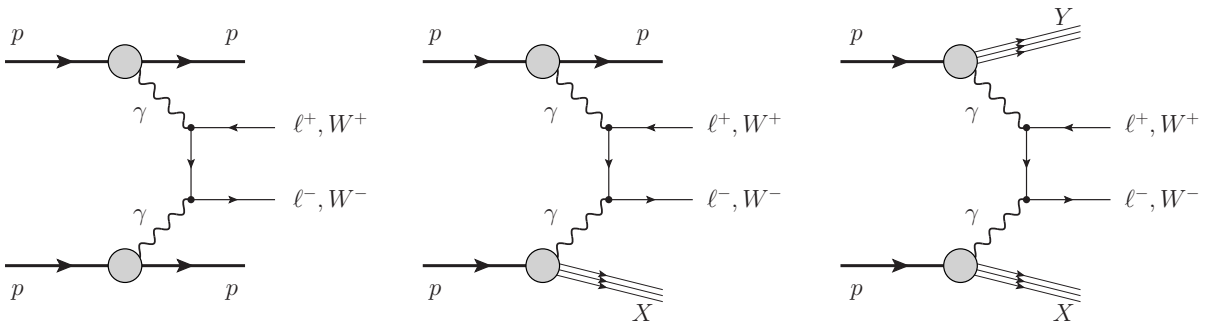

Figure 18. Two-photon particle production in elastic (left), semielastic (center) and inelastic (right) processes.

in pp collisions assuming that the cross section for $\sigma_{\gamma p \to V p}$ was given by the H1 fit [124]

$$\sigma_{\gamma p \to J/\Psi p}(W_{\gamma p}) = N \left(\frac{W_{\gamma p}}{90\text{GeV}} \right)^{\lambda} \tag{27}$$

where $N = 81 \pm 3$ nb and $\lambda = 0.67 \pm 0.03$. Moreover, for the Υ production, we assumed that $\sigma_{\gamma p \to \Upsilon p} = (0.12\text{pb})(W_{\gamma p}/W_0)^{1.6}$ with $W_0 = 1$ GeV, as given in Ref. [19].

In order to estimate the diffractive quarkonium photoproduction associated to the inelastic component of the photon distribution we should to specify the hard scale μ^2. As can be verified in the literature, the choice of this scale is a bit ambiguous [117, 125, 126, 119, 120, 127]. In general it is assumed that it is related to the center-of-mass energy of the photon - induced subprocess or to a hard scale in the final state. Following previous analysis that demonstrate that the mass of the vector meson can be considered a hard scale which justifies a perturbative calculation of its photoproduction, in what follows we will assume that $\mu^2 = M_V^2$. It is important to emphasize that larger values of the hard scale increase our predictions, since the magnitude of the inelastic photon distribution is amplified by the DGLAP evolution. Moreover, in order to estimate the inelastic component using the Naive approach given by Eq. (25) we will assume that $\mu^2 = Q_1^2 = M_V^2$ and that the parton distributions are given by the MRST 2001 leading order parametrization [53]. In Fig. 17 we present our predictions for the rapidity distribution of

the diffractive J/Ψ and Υ photoproduction in pp collisions at $\sqrt{s} = 7$ (For more details see Ref. [30]). We consider three different models for the inelastic component of the photon distribution and also present the predictions associated to the elastic contribution for comparison. For the J/Ψ production, we obtain that at midrapidities the NNPDF predictions are a factor ≈ 1.5 smaller than the elastic one. On the other hand, the MRST2004QED predictions are larger than elastic one, with the Naive predictions being of the same order of the elastic one. The results presented in Ref. [30] indicated that inelastic predictions obtained using the MRST2004QED parametrization are larger than the elastic one in the full rapidity range. In contrast, the NNPDF parametrization implies that the inelastic contribution is larger than the elastic one at large rapidities. These behaviours are directly related to the x-dependence of the inelastic component of the photon distribution for $\mu^2 = M^2_{J/\Psi}$, since at large rapidities we are probing larger values of x. For the Υ production, we now obtain that at midrapidities the inelastic NNPDF prediction is of the same order than the elastic one. Moreover, we obtain that the inelastic predictions dominate at large rapidities.

Lets now review the results presented in Ref. [31], where we have proposed to probe the photon flux in two - photon interactions (For related studies see Refs. [133, 134]). Following Ref. [128] we will write the cross sections for the $\gamma\gamma$ production of a final state F ($= W^+W^-$ or $\mu^+\mu^-$) of invariant mass $M = W_{\gamma\gamma}$ in a factorized form:

$$\sigma = \mathcal{L}_{eff}(M^2, Y)\hat{\sigma}(M^2) \tag{28}$$

where $\hat{\sigma}$ is the cross section for the hard subprocess $\gamma\gamma \to F$ and $\mathcal{L}_{eff}$ is the effective photon - photon luminosity for the production of the system F at rapidity Y. The effective luminosity is given in terms of the photon distribution of the incident hadrons as follows

$$\frac{\partial \mathcal{L}_{eff}}{\partial Y \partial \ln M^2} = x_1\gamma(x_1, \mu^2) \cdot x_2\gamma(x_2, \mu^2) \ . \tag{29}$$

The photon distribution of a nucleon consist of two parts: the elastic and inelastic components. In the elastic case, we have the coherent emission of photons from the hadron, without the dissociation of the incident hadron. In contrast, in the inelastic case the photons are emitted by the quarks and antiquarks present in the hadrons, and the incident hadron is excited in a low-mass state. Consequently, we can define three different classes of $\gamma\gamma$ events: (a) the *elastic* processes, where the final state F is produced with the two incident hadrons remaining intact, and the effective luminosity is proportional to $x_1\gamma^{el}(x_1, \mu^2) \cdot x_2\gamma^{el}(x_2, \mu^2)$; (b) the *semielastic* processes, where one of the incident hadrons remain intact and the other dissociates, with $\mathcal{L}_{eff} \propto [x_1\gamma^{el}(x_1, \mu^2) \cdot x_2\gamma^{inel}(x_2, \mu^2) + x_1\gamma^{inel}(x_1, \mu^2) \cdot x_2\gamma^{el}(x_2, \mu^2)]$ and (c) *inelastic* processes, where the two incident hadrons dissociates and $\mathcal{L}_{eff} \propto x_1\gamma^{inel}(x_1, \mu^2) \cdot x_2\gamma^{inel}(x_2, \mu^2)$. These three classes are represented in Fig. 18. In all these processes, the final state will be characterized by the presence of the state F and two rapidity gaps, with the hadrons or the low-mass hadron beam fragments travelling in the beam direction.

In principle, these different processes can be separated by the tagging of the two very forward scattered hadrons and by the requirement of the presence of large rapidities gaps in the central detector. Unfortunately, forward detectors were not available during Run I of the LHC, and the next run starting in 2015 is going to produce a sizeable pile-up obliterating the observation of rapidity gaps. Therefore, experimental separation of those contributions is a hard task and demands better knowledge of final-state kinematics in an observed event. In Run I, the CMS Collaboration have separated the signal of two-photon production of pairs (W^+W^- and $\mu^+\mu^-$) by selecting lepton tracks from the information recorded in the tracking system, which can be used to analyze exclusive events even in a scenario with large number of interaction per bunch crossing (high pileup). Offline, events have been selected with no additional tracks associated

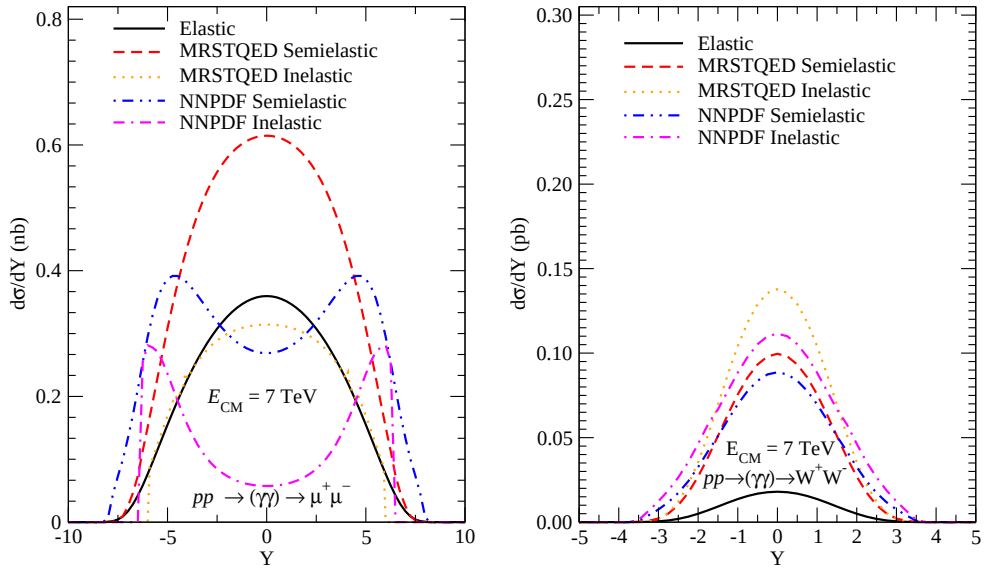

Figure 19. Rapidity and invariant mass distributions for the W^+W^- production considering the MRSTQED and NNPDF parametrizations. The prediction for elastic processes is presented for comparison.

to the $\ell^+\ell^-$ vertex. Since both elastic and non-elastic processes contribute in this case, we have higher photon luminosities, although larger uncertainties in the theoretical predictions, due to the lesser theoretically controlled inelastic photon flux. Currently, there is a great expectation due to the installation of the CMS-TOTEM Precision Proton Spectrometer (CT-PPS) [32], which will be setup in a first stage in one of the CMS sides at about 200 metres from the interaction point. Certainly, this new detector will improve the analysis of exclusive processes and allow us to access a variety of physics topics at high luminosities. However, a precise determination of the semielastic contribution will be still fundamental before the search of New Physics in two-photon processes.

Lets now estimate the rapidity and invariant mass dependencies of the cross sections for the $\mu^+\mu^-$ and W^+W^- production in two-photon interactions. In Fig. 19 we present our predictions for the rapidity distributions for the $\mu^+\mu^-$ (left panel) and W^+W^- production considering the MRSTQED and NNPDF parametrizations, as well as the prediction for elastic processes. In the case of $\mu^+\mu^-$ production we have that the MRSTQED and NNPDF predictions for the rapidity distributions differ significantly. In comparison to the elastic contribution, we have that the semielastic MRSTQED prediction dominates at central rapidities and the NNPDF one dominates for large values of rapidities, with the inelastic contribution being a factor ≈ 4 smaller for $Y = 0$ at $\sqrt{s} = 7$ TeV. Such distinct behaviours make the analysis of the rapidity distribution ideal to discriminate between the different models for the inelastic photon distribution. In Fig. 19 (right panel) we present the corresponding distributions for W^+W^- production. In this case the shape of the rapidity distributions predicted by the MRSTQED and NNPDF parametrizations are similar, differing only in its magnitudes, which are much larger than the prediction for elastic processes at central rapidities. Such dominance also is present in the invariant mass distributions.

The results presented in Ref. [31] and briefly reviewed in this Section demonstrated that the distinct models for the inelastic photon flux implies very distinct behaviours for the effective photon - photon luminosities and differential cross sections. It implies that the use of the two-

photon particle production mechanism to search rare events will be not a easy task before the determination of the correct description of the inelastic photon distribution. In particular, since in a first moment only one of the very forward detectors of CT-PPS will be installed, which would not eliminate the semielastic processes. Our results indicated that the analysis of the rapidity distribution for $\mu^+\mu^-$ production can be a discriminator among the possible models for the photon distribution. In particular, the determination of the distribution for central rapidities already differentiate the distinct models. Finally, we believe that the analyses carried out with the data of the two-photon production of pairs, in conjunction with the exclusive vector meson production discussed in Ref. [30], will allow us to precisely determine the adequate description of the photon distribution, which still is an important open question in High Energy Physics.

7. Conclusions

In this contribution we have discussed the photon induced interactions which can be analysed in hadronic colliders. In particular, we have demonstrated that several open questions which remain in the Standard Model can be studied at the LHC, assuming it as a photon collider. The recent experimental results obtained by RHIC and LHC colliders have demonstrated that the analysis of these interactions is feasible, which has motivated the theoretical improvement of the description of inclusive and exclusive photon - hadron interactions. Our results indicate that at the LHC we can probe the gluon distribution at small-x, the QCD dynamics, the Odderon, the production of Charmoniumlike exotic states and the photon flux of the proton. Such results demonstrate that photon induced interactions are an important laboratory for the hadronic physics.

Acknowledgments

I am very grateful to D. D'Enterria and V. Telnov for the invitation to attend to the International Conference PHOTON 2015. Moreover, I would like to congratulate the organizers for the stimulating and interesting meeting. I also wish to thank my collaborators, C. A. Bertulani, M. V. T. Machado, B. D. Moreira, F. S. Navarra, W. K. Sauter, M. L. L. Silva and G. G. da Silveira, with whom most of the work presented here was done over the years. This work was partially financed by the Brazilian funding agencies CNPq, CAPES and FAPERGS.

References

[1] C. Adler *et al.* [STAR Collaboration], Phys. Rev. Lett. **89**, 272302 (2002)
[2] S. Afanasiev *et al.* [PHENIX Collaboration], Phys. Lett. B **679**, 321 (2009)
[3] T. Aaltonen *et al.* [CDF Collaboration], Phys. Rev. Lett. **102**, 242001 (2009)
[4] B. Abelev *et al.* [ALICE Collaboration], Phys. Lett. B **718**, 1273 (2013)
[5] E. Abbas *et al.* [ALICE Collaboration], Eur. Phys. J. C **73**, 2617 (2013)
[6] R. Aaij *et al.* [LHCb Collaboration], J. Phys. G **40**, 045001 (2013)
[7] R. Aaij *et al.* [LHCb Collaboration], J. Phys. G **41**, 055002 (2014)
[8] R. Aaij *et al.* [LHCb Collaboration], JHEP **1509**, 084 (2015)
[9] S. Chatrchyan *et al.* [CMS Collaboration], JHEP **01**, 052 (2012)
[10] S. Chatrchyan *et al.* [CMS Collaboration], JHEP **11**, 080 (2012)
[11] S. Chatrchyan *et al.* [CMS Collaboration], JHEP **07**, 116 (2013)
[12] V. P. Goncalves and C. A. Bertulani, Phys. Rev. C **65**, 054905 (2002).
[13] A. L. Ayala Filho, V. P. Goncalves and M. T. Griep, Phys. Rev. C **78**, 044904 (2008)
[14] A. Adeluyi and C. Bertulani, Phys. Rev. C **84**, 024916 (2011); Phys. Rev. C **85**, 044904 (2012)
[15] V. Guzey and M. Zhalov, JHEP **1310**, 207 (2013); JHEP **1402**, 046 (2014).
[16] V. P. Goncalves and M. V. T. Machado, Eur. Phys. J. C **40**, 519 (2005).
[17] V. P. Goncalves and M. V. T. Machado, Phys. Rev. C **73**, 044902 (2006); Phys. Rev. D **77**, 014037 (2008); Phys. Rev. C **80**, 054901 (2009).
[18] V. P. Goncalves and M. V. T. Machado, Phys. Rev. C **84**, 011902 (2011)
[19] L. Motyka and G. Watt, Phys. Rev. D **78**, 014023 (2008)
[20] T. Lappi and H. Mantysaari, Phys. Rev. C **87**, 032201 (2013)

[21] M. B. Gay Ducati, M. T. Griep and M. V. T. Machado, Phys. Rev. D **88**, 017504 (2013); Phys. Rev. C **88**, 014910 (2013).
[22] V. P. Goncalves, B. D. Moreira and F. S. Navarra, Phys. Rev. C **90**, no. 1, 015203 (2014).
[23] V. P. Goncalves, B. D. Moreira and F. S. Navarra, Phys. Lett. B **742**, 172 (2015).
[24] W. Schafer and A. Szczurek, Phys. Rev. D **76**, 094014 (2007); A. Rybarska, W. Schafer and A. Szczurek, Phys. Lett. B **668**, 126 (2008); A. Cisek, W. Schafer and A. Szczurek, Phys. Rev. C **86**, 014905 (2012)
[25] V. P. Goncalves and M. M. Machado, Eur. Phys. J. C **72**, 2231 (2012)
[26] V. P. Goncalves and M. M. Machado, Eur. Phys. J. A **50**, 72 (2014)
[27] A. Cisek, W. Schafer and A. Szczurek, JHEP **1504**, 159 (2015)
[28] V. P. Goncalves, Nucl. Phys. A **902**, 32 (2013)
[29] V. P. Goncalves and W. K. Sauter, Phys. Rev. D **91**, no. 9, 094014 (2015)
[30] V. P. Goncalves and G. G. da Silveira, Phys. Rev. D **91**, no. 5, 054013 (2015)
[31] G. G. da Silveira and V. P. Goncalves, Phys. Rev. D **92**, no. 1, 014013 (2015)
[32] The CMS and TOTEM Collaborations, CMS-TOTEM Precision Proton Spectrometer Technical Design Report, http://cds.cern.ch/record/1753795.
[33] C. A. Bertulani and G. Baur, Phys. Rep. **163**, 299 (1988); G. Baur, K. Hencken, D. Trautmann, S. Sadovsky, Y. Kharlov, Phys. Rep. **364**, 359 (2002); V. P. Goncalves and M. V. T. Machado, Mod. Phys. Lett. A **19**, 2525 (2004); C. A. Bertulani, S. R. Klein and J. Nystrand, Ann. Rev. Nucl. Part. Sci. **55**, 271 (2005); K. Hencken *et al.*, Phys. Rept. **458**, 1 (2008).
[34] V. M. Budnev, I. F. Ginzburg, G. V. Meledin and V. G. Serbo, Phys. Rept. **15**, 181 (1975).
[35] F. Gelis, E. Iancu, J. Jalilian-Marian and R. Venugopalan, Ann. Rev. Nucl. Part. Sci. **60**, 463 (2010).
[36] K. J. Eskola, V. J. Kolhinen and P. V. Ruuskanen, Nucl. Phys. B **535**, 351 (1998); K. J. Eskola, V. J. Kolhinen and C. A. Salgado, Eur. Phys. J. C **9**, 61 (1999).
[37] D. de Florian and R. Sassot, Phys. Rev. D **69**, 074028 (2004).
[38] M. Hirai, S. Kumano and M. Miyama, Phys. Rev. D **64**, 034003 (2001); Phys. Rev. C **70**, 044905 (2004).
[39] M. Hirai, S. Kumano and T. H. Nagai, Phys. Rev. C **76**, 065207 (2007).
[40] K. J. Eskola, H. Paukkunen and C. A. Salgado, JHEP **0807**, 102 (2008).
[41] N. Armesto, J. Phys. G **32**, R367 (2006).
[42] K. J. Eskola, H. Paukkunen and C. A. Salgado, JHEP **0904**, 065 (2009).
[43] N. Baron and G. Baur, Phys. Rev. C **48**, 1999 (1993).
[44] S. R. Klein, J. Nystrand and R. Vogt, Eur. Phys. J. C **21**, 563 (2001); Phys. Rev. C **66**, 044906 (2002)-
[45] V. P. Goncalves and M. V. T. Machado, Eur. Phys. J. C **31**, 371 (2003) ; Phys. Rev. D **71**, 014025 (2005); Phys. Rev. C **73**, 044902 (2006); Phys. Rev. D **75**, 031502 (2007); V. P. Goncalves, M. V. T. Machado and A. R. Meneses, Phys. Rev. D **80**, 034021 (2009).
[46] V. P. Goncalves, Phys. Rev. D **88**, no. 5, 054025 (2013).
[47] M. Bedjidian *et al.*, arXiv:hep-ph/0311048.
[48] V. P. Goncalves and M. V. T. Machado, Eur. Phys. J. C **30**, 387 (2003); V. P. Goncalves, M. S. Kugeratski and F. S. Navarra, Phys. Rev. C **81**, 065209 (2010)
[49] V. P. Goncalves and M. V. T. Machado, Eur. Phys. J. C **32**, 501 (2004).
[50] F. -P. Schilling, Int. J. Mod. Phys. A **27**, 1230016 (2012)
[51] M. Glück and E. Reya, Phys. Lett. B **79**, 453 (1978).
[52] R. K. Ellis and P. Nason, Nucl. Phys. B **312**, 551 (1989); J. Smith and W. L. van Neerven, Nucl. Phys. B **374**, 36 (1992).
[53] A. D. Martin, R. G. Roberts, W. J. Stirling and R. S. Thorne, Eur. Phys. J. C **23**, 73 (2002)
[54] H. -L. Lai, M. Guzzi, J. Huston, Z. Li, P. M. Nadolsky, J. Pumplin and C. -P. Yuan, Phys. Rev. D **82**, 074024 (2010)
[55] D. d'Enterria and J. P. Lansberg, Phys. Rev. D **81**, 014004 (2010)
[56] J. C. Collins, L. Frankfurt and M. Strikman, Phys. Rev. D **56**, 2982 (1997)
[57] M. G. Ryskin, Z. Phys. C **57**, 89 (1993).
[58] S. J. Brodsky, L. Frankfurt, J. F. Gunion, A. H. Mueller and M. Strikman, Phys. Rev. D **50**, 3134 (1994).
[59] M. G. Ryskin, R. G. Roberts, A. D. Martin and E. M. Levin, Z. Phys. C **76**, 231 (1997)
[60] L. Frankfurt, W. Koepf and M. Strikman, Phys. Rev. D **57**, 512 (1998)
[61] A. D. Martin, C. Nockles, M. G. Ryskin and T. Teubner, Phys. Lett. B **662**, 252 (2008)
[62] D. Y. Ivanov, A. Schafer, L. Szymanowski and G. Krasnikov, Eur. Phys. J. C **34**, 297 (2004)
[63] A. D. Martin, M. G. Ryskin and T. Teubner, Phys. Lett. B **454**, 339 (1999)
[64] C. Adloff *et al.* [H1 Collaboration], Phys. Lett. B **483**, 23 (2000).
[65] S. Chekanov *et al.* [ZEUS Collaboration], Eur. Phys. J. C **24**, 345 (2002).
[66] J. Breitweg *et al.* [ZEUS Collaboration], Phys. Lett. B **437**, 432 (1998).
[67] Y. V. Kovchegov and E. Levin, "Quantum chromodynamics at high energy ", Cambridge monographs on

particle physics, nuclear physics and cosmology, 33 Cambridge, UK: Cambridge Univ. Pr. (2012)
[68] I. I. Balitsky, Nucl. Phys. **B463**, 99 (1996); Phys. Rev. Lett. **81**, 2024 (1998); Phys. Rev. D **60**, 014020 (1999)
[69] J. Jalilian-Marian, A. Kovner, L. McLerran and H. Weigert, Phys. Rev. D **55**, 5414 (1997); J. Jalilian-Marian, A. Kovner and H. Weigert, Phys. Rev. D **59**, 014014 (1999), *ibid.* **59**, 014015 (1999), *ibid.* **59** 034007 (1999); A. Kovner, J. Guilherme Milhano and H. Weigert, Phys. Rev. D **62**, 114005 (2000); H. Weigert, Nucl. Phys. **A703**, 823 (2002); E. Iancu, A. Leonidov and L. McLerran, Nucl.Phys. **A692**, 583 (2001); E. Ferreiro, E. Iancu, A. Leonidov and L. McLerran, Nucl. Phys. **A701**, 489 (2002).
[70] Y.V. Kovchegov, Phys. Rev. D **60**, 034008 (1999); Phys. Rev. D **61**, 074018 (2000).
[71] N. N. Nikolaev, B. G. Zakharov, Phys. Lett. B **332**, 184 (1994); Z. Phys. C **64**, 631 (1994).
[72] H. Kowalski, L. Motyka and G. Watt, Phys. Rev. D **74**, 074016 (2006)
[73] N. Armesto and A. H. Rezaeian, Phys. Rev. D **90**, no. 5, 054003 (2014)
[74] J. Bartels, K. Golec-Biernat and K. Peters, Acta Phys. Polon. B **34**, 3051 (2003)
[75] H. G. Dosch, T. Gousset, G. Kulzinger and H. J. Pirner, Phys. Rev. **D55**, 2602 (1997).
[76] J. Nemchik, N. N. Nikolaev, E. Predazzi and B. G. Zakharov, Z. Phys. C **75**, 71 (1997)
[77] J. R. Forshaw, R. Sandapen and G. Shaw, Phys. Rev. D **69**, 094013 (2004)
[78] H. Kowalski and D. Teaney, Phys. Rev. D **68**, 114005 (2003)
[79] J. L. Albacete, N. Armesto, J. G. Milhano and C. A. Salgado, Phys. Rev. **D80**, 034031 (2009).
[80] K. Golec-Biernat and M. Wusthoff, Phys. Rev. D **59**, 014017 (1999) .
[81] E. Iancu, K. Itakura, S. Munier, Phys. Lett. **B590**, 199 (2004).
[82] V. P. Goncalves, M. S. Kugeratski, M. V. T. Machado and F. S. Navarra, Phys. Lett. B **643**, 273 (2006).
[83] G. Watt and H. Kowalski, Phys. Rev. D **78**, 014016 (2008)
[84] A. Rezaeian and I. Schmidt, Phys. Rev. D **88**, 074016 (2013)
[85] M. Kozlov, A. Shoshi and W. Xiang, JHEP **0710**, 020 (2007)
[86] L. N. Lipatov, Sov. J. Nucl. Phys. **23**, 338 (1976); E. A. Kuraev, L. N. Lipatov and V. S. Fadin, Sov. Phys. JETP **44**, 443 (1976); *ibid.* **45**, 199 (1977); I. I. Balitsky and L. N. Lipatov, Sov. J. Nucl. Phys. **28**, 822 (1978).
[87] J. Bartels, Nucl. Phys. B **175**, 365 (1980); J. Kwiecinski and M. Praszalowicz, Phys. Lett. B **94**, 413 (1980).
[88] C. Ewerz, hep-ph/0306137.
[89] L. D. Faddeev and G. P. Korchemsky, Phys. Lett. B **342**, 311 (1995); G. P. Korchemsky, Nucl. Phys. B **443**, 255 (1995)
[90] J. Wosiek and R. A. Janik, Phys. Rev. Lett. **79**, 2935 (1997); Phys. Rev. Lett. **82**, 1092 (1999).
[91] J. Bartels, L. N. Lipatov and G. P. Vacca, Phys. Lett. B **477**, 178 (2000)
[92] J. Bartels, M. A. Braun, D. Colferai and G. P. Vacca, Eur. Phys. J. C **20**, 323 (2001)
[93] J. Czyzewski, J. Kwiecinski, L. Motyka and M. Sadzikowski, Phys. Lett. B **398**, 400 (1997) [Erratum-ibid. B **411**, 402 (1997)]; R. Engel, D. Y. .Ivanov, R. Kirschner and L. Szymanowski, Eur. Phys. J. C **4**, 93 (1998).
[94] H. Cheng and T. T. Wu, Phys. Rev. Lett. **22**, 666 (1969); Phys. Rev. **182**, 1852 (1969); *ibid.* **182**, 1868 (1969); *ibid.* **182**, 1873 (1969); *ibid.* **182**, 1899 (1969).
[95] H. G. Dosch, C. Ewerz and V. Schatz, Eur. Phys. J. C **24**, 561 (2002)
[96] S. J. Brodsky, F. Fleuret, C. Hadjidakis and J. P. Lansberg, Phys. Rept. **522**, 239 (2013)
[97] N. Brambilla, S. Eidelman, B. K. Heltsley, R. Vogt, G. T. Bodwin, E. Eichten, A. D. Frawley and A. B. Meyer *et al.*, Eur. Phys. J. C **71**, 1534 (2011)
[98] M. Nielsen, F. S. Navarra and S. H. Lee, Phys. Rep. **497**, 41 (2010)
[99] M. Nielsen and F. S. Navarra, Mod. Phys. Lett. A**29**, 1430005 (2014).
[100] C. Bignamini, B. Grinstein, F. Piccinini, A. D. Polosa and C. Sabelli, Phys. Rev. Lett. **103**, 162001 (2009); P. Artoisenet and E. Braaten, Phys. Rev. D **81**, 114018 (2010); A. Ali and W. Wang, Phys. Rev. Lett. **106**, 192001 (2011); A. Esposito, F. Piccinini, A. Pilloni and A. D. Polosa, J. Mod. Phys. **4**, 1569 (2013); F. -K. Guo, U. -G. Meiner and W. Wang, arXiv:1308.0193 [hep-ph].
[101] S. Cho *et al.* [ExHIC Collaboration], Phys. Rev. Lett. **106**, 212001 (2011); Phys. Rev. C **84**, 064910 (2011); Nucl. Phys. A **914**, 377 (2013).
[102] X. H. Liu, Q. Zhao and F. E. Close, Phys. Rev. D**77**, 094005 (2008).
[103] J. He and X. Liu, Phys. Rev. D**80**, 114007 (2009).
[104] Q. Y. Lin, X. Liu and H. S. Xu, Phys. Rev. D**88**, 114009 (2013).
[105] Q. Y. Lin, X. Liu and H. S. Xu, Phys. Rev. D**89**, 034016 (2014).
[106] V. P. Goncalves, D. T. da Silva and W. K. Sauter, Phys. Rev. C **87**, 028201 (2013)
[107] C. A. Bertulani, Phys. Rev. C **79**, 047901 (2009).
[108] V. P. Goncalves and M. L. L. da Silva, Phys. Rev. D **89**, no. 11, 114005 (2014)
[109] T. Bauer R. D. Spital, D. R. Yennie and F. M. Pipkin, Rev. Mod. Phys. **50**, 261 (1978).
[110] L. Maiani, V. Riquer, R. Faccini, F. Piccinini, A. Pilloni and A. D. Polosa, Phys. Rev. D **87**, no. 11, 111102

(2013)
[111] P. V. Landshoff and O. Nachtmann, Z. Phys. C **35**, 405 (1987).
[112] E. Fermi, Z. Phys. **29**, 315 (1924).
[113] E. J. Williams, Phys. Rev. **45**, 729 (1934).
[114] C. F. von Weizsacker, Z. Phys. **88**, 612 (1934).
[115] B. A. Kniehl, Phys. Lett. B **254**, 267 (1991).
[116] A. De Rujula and W. Vogelsang, Phys. Lett. B **451**, 437 (1999)
[117] M. Drees, R. M. Godbole, M. Nowakowski and S. D. Rindani, Phys. Rev. D **50**, 2335 (1994)
[118] M. Gluck, C. Pisano and E. Reya, Phys. Lett. B **540**, 75 (2002); C. Pisano, hep-ph/0512306.
[119] A. D. Martin, R. G. Roberts, W. J. Stirling and R. S. Thorne, Eur. Phys. J. C **39**, 155 (2005)
[120] R. D. Ball *et al.* [NNPDF Collaboration], Nucl. Phys. B **877**, 290 (2013)
[121] C. Schmidt, J. Pumplin, D. Stump and C.-P. Yuan, PoS DIS **2014**, 054 (2014).
[122] A. D. Martin and M. G. Ryskin, Eur. Phys. J. C **74**, 3040 (2014)
[123] M. Drees and D. Zeppenfeld, Phys. Rev. D **39**, 2536 (1989).
[124] C. Adloff *et al.* [H1 Collaboration], Phys. Lett. B **541**, 251 (2002); C. Alexa *et al.* [H1 Collaboration], Eur. Phys. J. C **73**, no. 6, 2466 (2013)
[125] J. Ohnemus, T. F. Walsh and P. M. Zerwas, Phys. Lett. B **328**, 369 (1994)
[126] G. Bhattacharya, P. Kalyniak and K. A. Peterson, Phys. Rev. D **53**, 2371 (1996)
[127] M. Luszczak and A. Szczurek, arXiv:1309.7201 [hep-ph].
[128] V. A. Khoze, A. D. Martin and M. G. Ryskin, Eur. Phys. J. C **23**, 311 (2002)
[129] S. R. Klein, J. Nystrand, Phys. Rev. C **60**, 014903 (1999).
[130] L. Frankfurt, M. Strikman and M. Zhalov, Phys. Lett. B **540**, 220 (2002).
[131] L. Frankfurt, M. Strikman and M. Zhalov, Phys. Lett. B **537**, 51 (2002); Phys. Rev. C **67**, 034901 (2003); L. Frankfurt, V. Guzey, M. Strikman and M. Zhalov, JHEP **0308**, 043 (2003).
[132] S. R. Klein, J. Nystrand, Phys. Rev. Lett. **92**, 142003 (2004).
[133] G. G. da Silveira, L. Forthomme, K. Piotrzkowski, W. Schfer and A. Szczurek, JHEP **1502**, 159 (2015)
[134] M. Luszczak, A. Szczurek and C. Royon, JHEP **1502**, 098 (2015)